Organic Geochemistry 182 (2023) 104641

Contents lists available at ScienceDirect

Organic Geochemistry

journal homepage: www.elsevier.com/locate/orggeochem

Compound-specific carbon isotope measurements of individual lipid biomarkers from immature Ediacaran rocks of Baltica

K. Pehr [a,b,*], A.A. Baczynski [c], A. Bekker [a,d], A. Hoffmann [a], K.H. Freeman [c], S.W. Poulton [e], G.D. Love [a]

[a] Department of Earth & Planetary Sciences, University of California, Riverside, CA 92521, USA
[b] Department of Earth and Environmental Sciences, Lehigh University, Bethlehem, PA 18015, USA[1]
[c] Department of Geosciences, Pennsylvania State University, University Park, PA 16802, USA
[d] Department of Geology, University of Johannesburg, Auckland Park 2006, South Africa
[e] School of Earth and Environment, University of Leeds, Leeds LS2 9JT, UK

ARTICLE INFO

Associate Editor–**Rienk Smittenberg**

Keywords:
Compound-specific isotope analysis
Stable carbon isotopes
Epicontinental seas
Ediacaran
Hopanes
Steranes
Baltica

ABSTRACT

Compound-specific carbon isotope ratios (CSIA) were measured for a suite of lipid biomarker compounds extracted from immature, late Ediacaran sedimentary rocks from drill cores sampled across Baltica. Using a newly developed picomolar-scale CSIA (pico-CSIA) method, we measured carbon isotope compositions of the abundant *n*-alkanes and hopanes, as well as C_{29} sterane, pristane, and phytane. Total organic carbon (TOC) of the Kotlin Regional Horizon in Baltica (Saint Petersburg area, Utkina Zavod drill core), from a low-salinity coastal environment, is consistently enriched in ^{13}C by up to 10‰, compared to that for Redkino and Kotlin marine rocks from other locations in Baltica. This ^{13}C enrichment is also recorded by the *n*-alkanes, hopanes, phytane, and C_{29} sterane. In all locations, the $\delta^{13}C$ values of the C_{29} sterane are within 2‰ of the bacterial hopane $\delta^{13}C$ values and within 0.7‰ of $\delta^{13}C_{TOC}$, suggesting that the abundant hopanes within these sediments could be derived from RuBisCO Calvin-Benson-Bassham pathway-utilizing organisms, as well as from bacterial heterotrophs. Since $\delta^{13}C_{lipid}$ signature tracks $\delta^{13}C_{TOC}$ values for the Kotlin Regional Horizon samples from Utkina Zavod location, the significant ^{13}C enrichments in this interval reflect either the $\delta^{13}C$ composition of DIC used for autotrophy or a muted magnitude of carbon isotope fractionation during lipid biosynthesis, but are not due to enhanced preservation of organic compounds and geopolymers derived from ^{13}C-enriched biochemicals. Pico-CSIA and biomarker data provide evidence for both regional environmental heterogeneity and secular changes in carbon cycling during deposition of sediments of the Kotlin and Redkino Regional Horizon intervals.

1. Introduction

The total organic carbon (TOC) isotope composition ($\delta^{13}C_{TOC}$) of ancient sedimentary rocks reflects the overall balance of the organic matter (OM) contributions from source organisms, the taphonomy of molecular preservation during diagenesis and long-term burial (e.g., selective preservation under oxic versus more reducing redox conditions), and the carbon isotope composition of the dissolved inorganic carbon (DIC) pool within the local depositional setting (Hayes et al., 1990; Freeman, 2001). While broad changes in $\delta^{13}C_{TOC}$ over geological time can represent global perturbations to the carbon cycle, including changes to the fraction of organic carbon burial and atmospheric pCO_2 concentrations, ecological and environmental factors pertinent to the local depositional setting often have a greater influence (Pagani et al., 1999; Pancost et al., 2013; Holtvoeth et al., 2019). CSIA can help disentangle this complex web of biogenic inputs and preservation effects on bulk $\delta^{13}C_{TOC}$ by constraining OM source influences on $\delta^{13}C_{TOC}$ and informing on the pathways of carbon acquisition for different biomarker compounds and their parent biota (Hayes, 2001; Pancost and Damsté, 2003).

There is a protracted increase in the abundance and diversity of eukaryotic organisms in the marine realm throughout the end of the Neoproterozoic Era (1000–541 Ma). The oceans of the Mesoproterozoic were bacterially dominated. However, during the late Tonian-

* Corresponding author at: Department of Earth and Environmental Sciences, Lehigh University, Bethlehem, PA 18015, USA.
E-mail address: kep220@leigh.edu (K. Pehr).
[1] Present address.

https://doi.org/10.1016/j.orggeochem.2023.104641
Received 10 February 2023; Received in revised form 23 June 2023; Accepted 27 June 2023
Available online 29 June 2023
0146-6380/© 2023 The Author(s). Published by Elsevier Ltd. This is an open access article under the CC BY license (http://creativecommons.org/licenses/by/4.0/).

Cryogenian Period (820–635 Ma) eukaryotes increased in their ecological abundance (Brocks et al., 2017; Zumberge et al., 2020). The most common early-mid Neoproterozoic eukaryotes were likely red algae and unicellular heterotrophs, as gauged from the dominance of cholestane amongst the total detectable C_{27}-C_{30} steranes (Brocks et al., 2017; Zumberge et al., 2020), with lower amounts of C_{28} steranes (ergostane and cryostane), and a dearth of C_{29} steranes (Zumberge et al., 2020). Following the Sturtian glaciation, green algae replaced red algae as the dominant eukaryotic primary producers, and these eukaryotes rivaled bacteria in terms of biomass production within the oceans (Love et al., 2009; Brocks et al., 2017; Hoshino et al., 2017). However, even by the end of the Ediacaran, in contrast to deep-water, open-marine settings, the contemporaneous Ediacaran sedimentary strata from Baltica, deposited in shallow-marine, epicontinental basins, show bacterially dominated biomarker assemblage patterns and consistently low TOC contents (Pehr et al., 2018; Goryl et al., 2018; Bobrovskiy et al., 2020). Much higher algal productivity was sustained during petroleum source rock deposition in the South Oman Salt basin (Grosjean et al., 2009; Love et al., 2009; Lee et al., 2015) and East Siberia (Kelly et al., 2011), where eutrophic conditions persisted over extended intervals of Ediacaran time. These biomarker distribution differences strongly imply that there was significant biological and chemical heterogeneity in the oceans affecting the relative bacterial and eukaryotic contributions to microbial ecology in different marine locations. This is expected for both modern and ancient ocean systems due to geographically variable biogeochemical cycling and nutrient availability.

One enigmatic geochemical signal found in the Proterozoic sedimentary rocks and oils derived from these source rocks, that has been linked to the rise of eukaryotes, is a switch in the relative carbon isotopic ordering of *n*-alkanes versus the acyclic isoprenoids, pristane (2,6,10,14-tetramethylpentadecane;$C_{19}H_{40}$;Pr) and phytane (2,6,10,14-tetramethylhexadecane;$C_{20}H_{42}$;Ph) (Logan et al., 1995, 1997). Many Neoproterozoic samples are characterized by an 'inverse ordering', where $\delta^{13}C$ of pristane and phytane is more negative with respect to that of *n*-alkanes and bulk OM (Logan et al., 1995, 1997; Close et al., 2011). Phanerozoic samples, as well as some of the younger Ediacaran samples, often show the opposite trend, where the sedimentary total organic carbon (TOC) consisting largely of kerogen has more positive $\delta^{13}C$ values typically 3-8‰ relative to those of *n*-alkanes and 1-5‰ relative to pristane and phytane (Hayes, 2001; Corso et al., 2012; Jaraula et al., 2013; Fox et al., 2020). This isotopic ordering in most Phanerozoic samples reflects the isotopic pattern originating from isotope fractionations in biosynthesis with organisms commonly using the RuBisCO Calvin-Benson-Bassham (RuBisCO-CBB) metabolic pathway for autotrophic carbon acquisition (Hayes, 2001), which accounts for most of the primary productivity in modern oceans (Pearson, 2010).

Logan et al. (1997) proposed that the ^{13}C-enriched *n*-alkanes relative to pristane, phytane, and bulk OM in Proterozoic sediments may be a consequence of intense microbial heterotrophic reworking of lipids with linear chains in the water column where high dissolved organic matter (DOM) concentrations were sustained. The ecological rise of macroscopic, multicellular eukaryotes and, eventually, the packaging of OM into fecal pellets may have facilitated increased sinking rates of OM, which could have significantly muted the impact of intensive water column heterotrophy starting at the late Ediacaran to early Phanerozoic transition. However, modeling by Close et al. (2011) suggested instead that an alternative explanation for such appreciably ^{13}C-enriched *n*-alkanes might be a large difference in isotope fractionation between small-sized bacterial producers and large-sized eukaryotic primary producers (Popp et al., 1998). An important caveat to this rationale is whether source contribution from archaea, including methanogens and methanotrophs, to the acyclic isoprenoids, was significant. This would complicate the interpretation of molecular isotopic ordering patterns, since pristane and phytane may be derived from biogenic sources other than chlorophyll pigments from photoautotrophs such as cyanobacteria and/or algae, which is usually their assumed major source.

Here, we report the results of the first detailed CSIA study on individual Ediacaran biomarkers from rocks that have undergone only a mild thermal history. These biomarker hydrocarbons were obtained via solvent extraction from a suite of thermally immature, organic carbon-lean siliciclastic sediments sampled from drill cores across Baltica (Russia and Ukraine). These sediments were likely deposited under widespread and protracted oligotrophic conditions that were seemingly persistent in different locations across Baltica (Pehr et al., 2018; Goryl et al., 2018) from the late Ediacaran through to the Early Cambrian. Using the newly developed picomolar-scale CSIA (Baczynski et al., 2018), we were able to measure $\delta^{13}C$ signatures for the major *n*-alkane and hopane compounds, as well as other individual biomarker alkanes, including C_{29} sterane (αααR), pristane, and phytane. Through this approach, we could assess the magnitude of the secular variations in $\delta^{13}C$ values for bulk sedimentary OM, as well as for individual lipid biomarkers in the same samples, within studied drill cores. Additionally, we could compare the organic carbon isotopic systematics for the same stratigraphic intervals from drill cores from numerous locations across Baltica, to assess the extent of regional heterogeneity, through this important interval in Earth history.

2. Materials and methods

2.1. Geological setting and samples

Baltica hosts the most thermally immature Ediacaran rocks reported worldwide for this time interval (Goryl et al., 2018; Pehr et al., 2018). A subset of late Ediacaran and Early Cambrian samples was selected from the suite of thermally immature samples used in a previous study for detailed biomarker analysis (Pehr et al., 2018). The sedimentary rocks were collected from the Utkina Zavod and Lugovoe drill cores located near St. Petersburg in the northeastern part of the Baltic monocline, the Gavrilov-Yam-1 drill core from the Moscow basin, the 4592 drill core from the Volyn region of Ukraine, and the 3628 drill core of the Podillya basin in southwestern Ukraine (Fig. 1, Table 1). The samples encompass strata from the Redkino, Kotlin, and Lontova Regional horizons. Detailed locations and descriptions of these samples, with geochemical screening data, have been reported previously (Pehr et al. 2018).

The age of the Redkino Regional Stage is now well-constrained by high-precision U-Pb Thermal Ionization Mass Spectrometry (TIMS) dates from White Sea, Russia and the Podillya basin in Ukraine at ca. 556 Ma (Martin et al., 2000; Soldatenko et al., 2019). By contrast, the age of the younger Kotlin Regional Horizon is not well-constrained geochronologically, but is mostly considered to represent the terminal ~ 10 million years of the Ediacaran Period (Grazhdankin et al., 2011; Meidla, 2017). Recently, an Early Cambrian age has been suggested for the Kotlin Regional Stage based on detrital zircon dates for sandstones from the Kanyliv Group in the Podillya basin in Ukraine (Paszkowski et al., 2021), and the Kotlin Regional Horizon in the Saint Petersburg and Ladoga areas of Russia (Ivleva et al., 2016, 2018; Ershova et al., 2019). These data were produced by the LA-ICP-MS method and so should be further verified with the CA-ID-TIMS method to check for potential Pb loss, which may result in younger dates. Importantly, *Harlaniella podolica* and *Vendotaenia antiqua Gnil.* that are common in the Kotlin Regional Horizon of Baltica are unknown in the Early Cambrian deposits. We therefore use the conventional late Ediacaran age assignment for the Kotlin Regional Horizon in this study.

Rock-Eval pyrolysis parameters (particularly low T_{max} values) and biomarker stereoisomer ratios are self-consistent in indicating that these sedimentary rocks are all thermally immature (Pehr et al., 2018). The drill-core samples from Utkina Zavod, Lugovoe, and the Volyn and Podillya basins (Table 1) correspond to a pre-oil window stage of maturity. Samples from the Gavrilov Yam-1 drill core and the 16PL outcrops are within the oil window, but at a maturity level prior to peak oil generation (Pehr et al., 2018). Analysis of the kerogen-bound hydrocarbons for these samples (Pehr et al., 2018) indicated that this

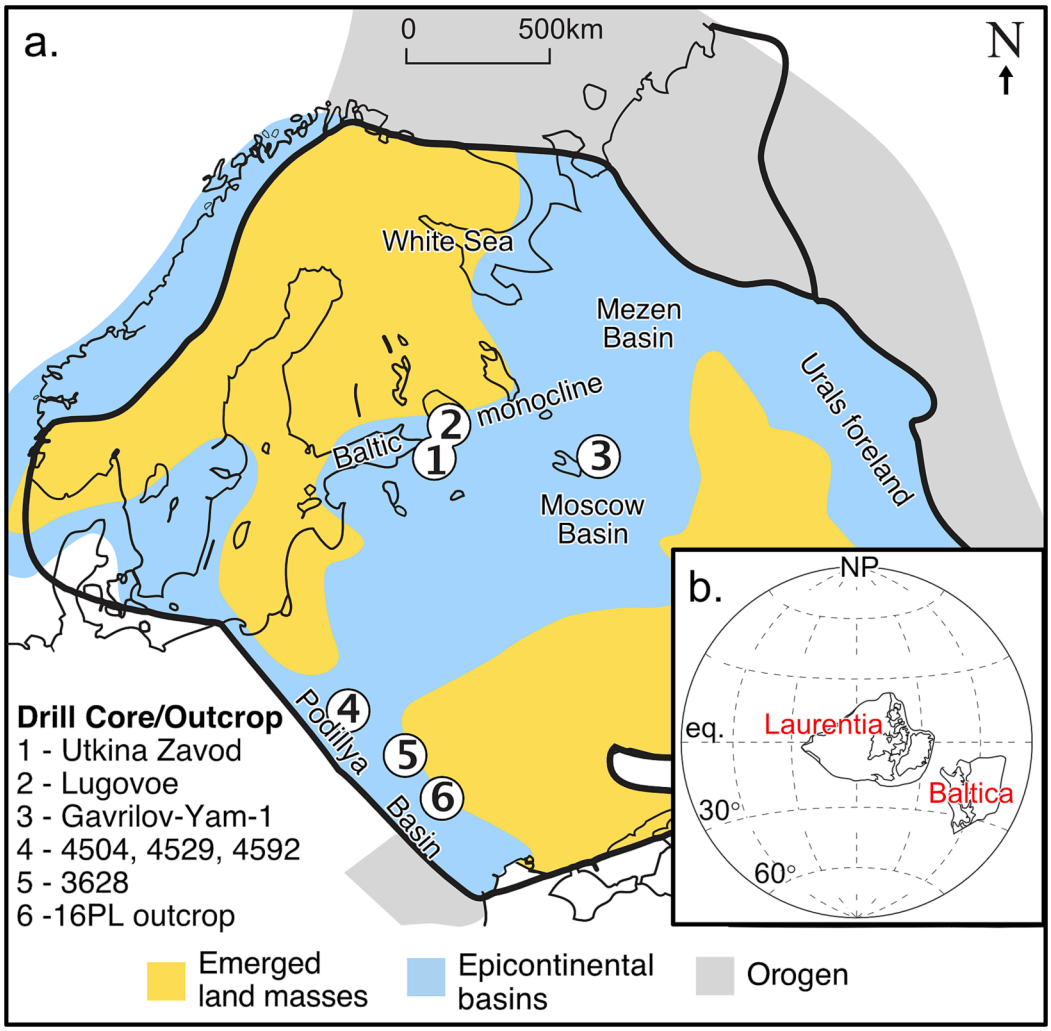

Fig. 1. (a) Paleogeographic reconstruction of Baltica during the late Ediacaran (modified from Sliaupa et al. 2006; Pehr et al., 2018) with drill cores and outcrop locations labeled; (b) Global reconstruction of Laurentia and Baltica at ca. 550 Ma, modified from Fedorova et al. (2013).

immature biomarker profile for steranes and hopanes is also preserved in the kerogen phase, confirming that the exceptionally immature polycyclic alkanes found in our bitumen extracts are primary and genuine Ediacaran biomarkers. Similar biomarker distribution profiles for immature Ediacaran rocks from Baltica have also been reported in another study and interpreted as predominantly endogenous lipid biomarker signals (Goryl et al., 2018).

2.2. Lipid biomarker analysis.

Rock samples (ranging from 5 to 20 g) were cut, pulverized, and solvent extracted, followed by separation of the bitumen extracts into three constituent fractions: aliphatic hydrocarbons, aromatics, and polar fractions, as previously described in detail (Pehr et al., 2018). Aliphatic and aromatic hydrocarbon fractions were analyzed using gas chromatography–mass spectrometry (GC–MS). Aliphatic hydrocarbons were also analyzed by metastable reaction monitoring (MRM)–GC–MS on a Waters Autospec Premier mass spectrometer for examination of polycyclic biomarker stereoisomer patterns in more detail. Standardized and proven analytical procedures were employed to prevent and check for contribution of contaminants to the rock bitumens. The immature downcore biomarker patterns, with the *n*-alkane, hopane, and sterane compound distributions ($C_{27hopane}$ Ts/(Ts + Tm) < 0.26 and $C_{31hopane}$ αβ 22S/(S + R) < 0.6) and the polycyclic biomarker dominance are consistent with the thermal immaturity of the rocks indicated by Rock-Eval pyrolysis parameters. The aliphatic hydrocarbon fractions were analyzed to generate total ion chromatograms (Fig. 2) in full-scan mode (monitoring from *m/z* 50 to 800) using gas chromatography–mass spectrometry (GC–MS) with an Agilent 7890A GC system coupled to an Agilent 5975C inert MSD mass spectrometer. The GC temperature program for full-scan analysis (*m/z* 50 to 800) was 60 °C (held for 2 min), heated to 150 °C at 20 °C /min, then to 325 °C at 2 °C /min, and held at 325 °C for 20 min. The gas chromatograph was equipped with a DB1-MS capillary column (60 m × 0.32 mm, 0.25-μm film thickness) and helium was used as a carrier gas.

To determine accurate molecular biomarker ratios (Table 1), aliphatic hydrocarbons were also analyzed by metastable reaction monitoring (MRM)–GC–MS on a Waters Autospec Premier mass spectrometer equipped with an Agilent 7890A gas chromatograph and DB-1MS coated capillary column (60 m × 0.25 mm, 0.25-μm film thickness), using He as a carrier gas to investigate polycyclic biomarker stereoisomer patterns in more detail. The GC temperature program started with an initial hold at 60 °C for 2 min, then heated to 150 °C at 10 °C /min rate, followed by 320 °C at 3 °C /min rate, and a final hold for 22 min. Analyses were performed via splitless injection in an electron-impact mode, with an ionization energy of 70 eV and an accelerating voltage of 8 kV. MRM ion-pair transitions were used for a suite of biomarker compounds (C_{27}–C_{35} hopanes, C_{31}–C_{36} methylhopanes, C_{19}–C_{26} tricyclic terpanes, C_{24} tetracyclic terpanes, C_{21}–C_{22} and C_{26}–C_{30} steranes, and C_{30} methylsteranes). Individual analyte peaks in rock

Table 1
Selected biomarker abundance ratios, bulk organic carbon isotope δ values and iron speciation redox proxies that provide biological and depositional environmental constraints.

Drill Core	Depth(m)	Location	Stage	Horizon	TOC (wt %)	C_{26}/C_{25} TT	FeHR/ FeT	Fepy/ FeHR	Hop/ Ster[1]	$\delta^{13}C_{TOC}$ (‰)
Utkina Zavod	64.15	Baltic Monocline	Late Ediacaran	Kotlin	0.42 [a]	2.32	0.28	0.06	3.4	−23.8 [a]
Utkina Zavod	71.67	Baltic Monocline	Late Ediacaran	Kotlin	0.34 [a]	2.15	0.30	0.07	1.6	−25.9 [a]
Utkina Zavod	87	Baltic Monocline	Late Ediacaran	Kotlin	0.27 [a]	1.9	0.27	0.00	3.9	−26.0 [a]
Utkina Zavod	111.6	Baltic Monocline	Late Ediacaran	Kotlin	0.67 [a]	2.78	0.47	0.01	3.2	−23.0 [a]
Utkina Zavod	119.9	Baltic Monocline	Late Ediacaran	Kotlin	0.40 [a]	1.79	0.17	0.00	7.7	−23.6 [a]
Utkina Zavod	124.6	Baltic Monocline	Late Ediacaran	Kotlin	0.52 [a]	2.28	0.24	0.02	3.6	−24.1 [a]
Utkina Zavod	127.8	Baltic Monocline	Late Ediacaran	Kotlin	0.76 [a]	1.91	n.d.	n.d.	7.5	−23.1 [a]
Utkina Zavod	152.8	Baltic Monocline	Late Ediacaran	Kotlin	0.31 [a]	1.56	0.20	0.02	4.8	−25.4 [a]
Utkina Zavod	153.5	Baltic Monocline	Late Ediacaran	Kotlin	0.27 [a]	1.71	0.65	0.00	5.0	−24.2 [a]
Utkina Zavod	162.1	Baltic Monocline	Late Ediacaran	Kotlin	0.44 [a]	1.63	0.15	0.09	5.0	−25.2 [a]
Utkina Zavod	171.4	Baltic Monocline	Late Ediacaran	Kotlin	0.21 [a]	2.10	0.24	0.02	4.0	−25.0 [a]
Lugovoe #13	41	Baltic Monocline	Late Ediacaran	Kotlin	0.48 [a]	1.24	0.92	0.53	7.2	−30.0 [a]
Lugovoe #13	44	Baltic Monocline	Late Ediacaran	Kotlin	0.44 [a]	1.09	0.64	0.17	8.3	−32.9 [a]
Lugovoe #13	47	Baltic Monocline	Late Ediacaran	Kotlin	0.51 [a]	1.46	0.55	0.19	2.0	−33.9 [a]
Lugovoe #13	71	Baltic Monocline	Late Ediacaran	Redkino	1.06 [a]	1.04	0.69	0.60	35.3	−33.1 [a]
Lugovoe #13	73	Baltic Monocline	Late Ediacaran	Redkino	0.85 [a]	0.97	0.78	0.55	73.4	−32.8 [a]
Lugovoe #13	75	Baltic Monocline	Late Ediacaran	Redkino	0.49 [a]	0.54	0.63	0.46	29.5	−29.6 [a]
Gavrilov Yam −1	1860	Moscow Syneclise	Cambrian	Lontova	0.23 [a]	0.66	0.34	0.03	27.8	−31.2 [a]
Gavrilov Yam −1	2018	Moscow Syneclise	Late Ediacaran	Kotlin	0.26 [a]	0.44	0.21	0.01	22.2	−25.2 [a]
4529	~195	Volyn basin	Late Ediacaran	Kotlin	0.12 [a]	1.03	0.60	0.01	22.8	−27.5 [a]
4529	~207	Volyn basin	Late Ediacaran	Kotlin	0.09 [a]	0.67	0.35	0.07	25.9	−27.0 [a]
4504	~200	Volyn basin	Late Ediacaran	Kotlin	0.13 [a]	0.61	0.32	0.03	22.5	−27.6 [a]
4592	~166	Volyn basin	Late Ediacaran	Redkino	0.47 [a]	1.44	0.63	0.25	119.2	−31.6 [a]
3628	226.5	Podillya basin	Late Ediacaran	Redkino	0.30 [a]	1.03	n.d.	n.d.	16.1	−29.0[b]
16PL	outcrop #22	Podillya basin	Late Ediacaran	Redkino	0.43 [a]	1.11	0.34	0.01	8.1	−26.8 [a]
16PL	outcrop #18	Podillya basin	Late Ediacaran	Redkino	0.18 [a]	1.13	0.33	0.00	11.1	−27.0 [a]
16PL	outcrop #11	Podillya basin	Late Ediacaran	Redkino	0.50 [a]	0.75	0.58	0.00	11.5	−24.0 [a]

[a] Previously reported in Pehr et al. (2018); isotope analyses were performed at Syracuse University[b] Isotopes analyses were performed at UCR[1]Hop/Ster is the ratio of major C_{27} - C_{35} hopane isomers/ C_{27} - C_{30} diasteranes and regular steranes; as previously reported in Pehr et al. (2018).

extract hydrocarbon fractions were quantified and found to constitute at least a three orders of magnitude larger signal than any trace peak detected in a full-laboratory blank using combusted sand. Procedural blanks with pre-combusted sand typically yielded <0.1 ng of individual hopane and sterane compounds per gram of combusted sand.

2.3. Bulk isotope analysis

Total organic carbon isotope analyses ($\delta^{13}C_{TOC}$) on samples marked with *b* in Table 1 were performed on samples using a Costech ECS 4010 Elemental Analyzer coupled to a Thermo Scientific Delta V Advantage isotope-ratio mass-spectrometer via a Thermo Scientific Conflo IV open-split gas interface system at UCR. 50–100 mg sample powders were acidified for at least 3 h using 12 N HCl in 50 mL centrifuge tubes; tubes were periodically vortexed. The tubes were then centrifuged at 2500 rpm for two minutes; acid was decanted, and powders were washed with deionized water. The process was repeated four times per sample to ensure removal of residual acid. Decarbonated and dried insoluble residues of ~ 5–10 mg were weighed into 9 × 10 mm tin boats for organic carbon isotope analysis. Combustion was achieved using a pulse of O_2 set for 60 s. The combustion and reduction columns were set to 1100 °C and 650 °C, respectively, with helium as the carrier gas at a flow rate of 100 mL/min. Isotope ratios are reported in standard (δ) delta notation relative to Vienna Pee Dee Belemnite where $\delta^{13}C_{org} = [[(^{13}C/^{12}C)_{sample}/(^{13}C/^{12}C)_{VPDB}] - 1] * 1000$. Average analytical precision of standard laboratory reference materials (Acetanilide, Hawaii glycine, and USGS SDO-1) used during analytical sessions was better than 0.10‰ for $\delta^{13}C_{org}$ values (1σ).

Bulk organic carbon isotope analysis on samples marked with *a* in Table 1 was performed on acidified rock powder residuals using an Elementar Isotope Cube elemental analyzer coupled to an Isoprime 100 isotope-mass-spectrometer as previously reported (Pehr et al., 2018). EA conditions were the following: helium purge was set for 30 s, oxidation and reduction reactor temperatures were 1100 °C and 650 °C, respectively, helium carrier gas flow was 230 mL/min, O_2 pulse was set for 60 s, and CO_2 trap was heated to 230 °C to release trapped sample CO_2. International reference materials (ANU sucrose [−10.4‰] and NIST 1547 peach leaves [−26.0‰]) were used to develop the correction scheme for sample data as described previously (Coplen et al., 2006). Reproducibility for samples and standards was better than ± 0.1‰.

2.4. Pico-compound specific carbon isotope analysis

Hydrocarbon fractions were analyzed using the pico-CSIA method for $\delta^{13}C$ measurements developed at Pennsylvania State University (Baczynski et al., 2018). The pico-CSIA method uses a Thermo Trace 1310 GC coupled to a Thermo MAT 253 IRMS via a GC Isolink (Baczynski et al., 2018 contains details). The gas chromatograph was fitted with a PTV injector that was held at 300 °C and operated in splitless mode. A fused silica capillary column (Agilent J&W DB-5, 10 m, 0.10 mm I.D., 0.10 μm film thickness) was used with helium as the carrier gas. The carrier gas had a programmed pressure method to ensure a consistent flow of ~ 0.48 mL/min throughout the run. The oven temperature program began at a temperature of 60 °C (held for 1.5 min), ramped to 230 °C at 100 °C /min (no hold) then to a maximum temperature of 320 °C at 40 °C /min with a final hold time of 5 min. The auxiliary gas pressure to the microfluidic splitter was held at 24 psi while solvent was vented, and then reduced to 18 psi while the GC effluent was directed to the IRMS.

Isotopic abundances were determined relative to a reference gas calibrated with Mix A (*n*-C_{16} to *n*-C_{30}; supplied by Arndt Schimmelmann, Indiana University). The $\delta^{13}C$ values were normalized to the standard Vienna Pee Dee Belemnite scale and are reported in standard delta notation. Standard errors of the mean for individual biomarker compounds range from 0.00‰ to 1.36‰ from repeat runs. Average standard errors for replicate sample analyses for individual *n*-alkanes were 0.22‰,

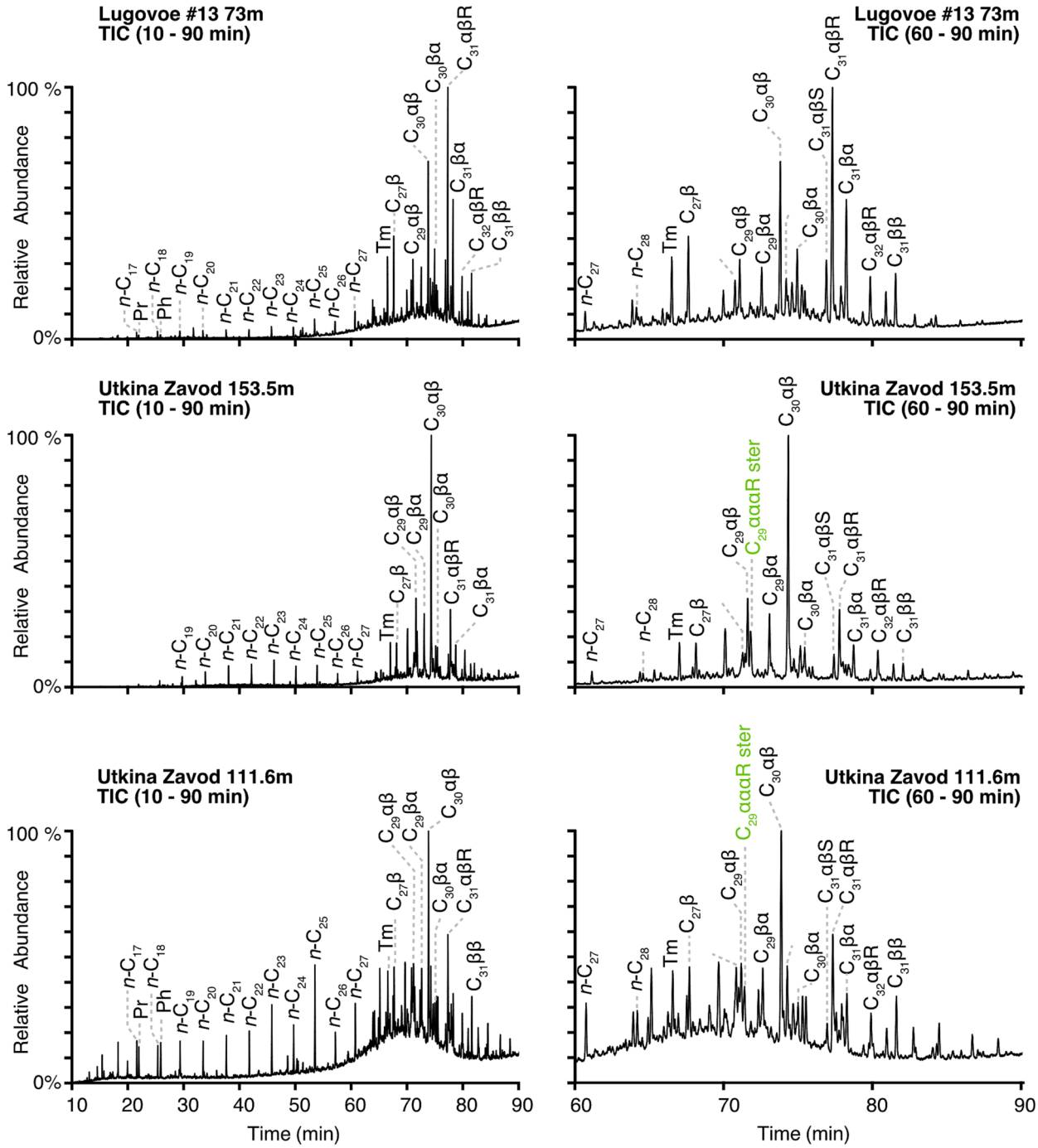

Fig. 2. Total ion chromatograms (TIC) for the extractable aliphatic hydrocarbons for the late Ediacaran sample Lugovoe #13 73 m, and the Early Cambrian samples Utkina Zavod 153.5 m and Utkina Zavod 111.6 m. The *n*-alkane series (n-C_{17} – n-C_{28}), pristane (Pr), phytane (Ph), C_{29} sterane 5α,14α,17α,20R-stigmastane (C_{29}αααR ster), and C_{27}–C_{31} hopanes denoted by their total carbon number and stereochemistry at C-17, C-21, and C-22 (e.g., C_{31}αβR), are all labeled. Hopanes are the most abundant series of biomarker alkanes in the aliphatic hydrocarbon fractions.

0.19‰ for phytane, and 0.28‰ for hopanes and C_{29} sterane (αααR).

2.5. Iron Speciation

Iron speciation was performed to gauge the environmental redox conditions by quantifying the total iron content of the rocks as well as contribution from iron minerals that are considered highly reactive (Fe_{HR}) to H_2S under anoxic conditions (Canfield et al., 1992; Poulton et al., 2004). Iron carbonate (Fe_{CARB}; including siderite and ankerite), ferric iron-(oxyhydr)oxide minerals (Fe_{OX}; including hematite and goethite), and magnetite (Fe_{MAG}), were separated following the sequential extraction technique described in Poulton and Canfield (2005). Pyrite (Fe_{py}) was determined stoichiometrically by weight from the Ag_2S precipitate formed after HCl and chromous chloride distillation (Canfield et al., 1986). These four iron phases combined make up the pool of Fe_{HR} (Poulton and Canfield, 2011). Fe_{HR} increases in concentration with respect to total iron (Fe_T) under anoxic water column conditions. $Fe_{HR}/Fe_T < 0.22$ may indicate oxic water column conditions, while $Fe_{HR}/Fe_T > 0.38$ commonly corresponds to anoxic conditions (Raiswell and Canfield, 1998; Raiswell et al., 2001; Poulton and

Canfield, 2011). The relative abundance of Fe_{py} is used to constrain the type of anoxia. For anoxic samples (i.e., $Fe_{HR}/Fe_T > 0.38$), $Fe_{py}/Fe_{HR} < 0.6$ suggests ferruginous (anoxic with dissolved Fe^{2+}) bottom water conditions, while euxinia (anoxic with free sulfide) is indicated when $Fe_{py}/Fe_{HR} > 0.6$–0.8 (Poulton, 2021).

3. Results

3.1. $\delta^{13}C_{TOC}$ and Compound-Specific Carbon Isotope Values

Bulk organic carbon isotope values ($\delta^{13}C_{TOC}$) for sedimentary OM were reported previously (Pehr et al., 2018) and show consistent stratigraphic trends for multiple sections across Baltica for the Redkino and Kotlin Regional horizons within single cores. Note that these bulk isotopic signatures vary markedly from location to location, which suggest they depend on prevailing environmental conditions in the ancient aquatic settings. Briefly summarized, for multiple samples from the Kotlin Regional Horizon from the Utkina Zavod drill core (Location 1 in Fig. 1), $\delta^{13}C_{TOC}$ values are significantly ^{13}C-enriched relative to typical Ediacaran marine OM, ranging from −26.0 to –23.0‰. Samples from the nearby Lugovoe drill core (Location 2 in Fig. 2) from the same Kotlin Regional Horizon are more depleted in ^{13}C, by up to 10‰, ranging from –33.9 to −30.0‰. These latter values are more typical for marine-sourced Ediacaran sedimentary organic matter, as found for Ediacaran source rocks from the South Oman Salt Basin (Grosjean et al., 2009, Lee et al., 2013).

Hopanes, *n*-alkanes and acyclic isoprenoids are the three most abundant series of resolvable biomarker compounds in the aliphatic hydrocarbon fractions (Fig. 2). The high relative abundance of polycyclic alkanes, such as hopanes and/or steranes, is typical for thermally immature (pre-oil window maturity) rocks of all geological ages, since dilution with abundant *n*-alkanes cleaved from kerogen and other macromolecules does not occur until a higher maturity level at the onset of catagenesis. The consistency in immature hydrocarbon patterns (Fig. 2) from systematic downcore sampling of the Utkina Zavod and Lugovoe drill-cores also confirms that these are genuine Ediacaran lipid biomarkers. CSIA of individual *n*-alkanes and hopane compounds reveals that $\delta^{13}C$ values of both compound classes generally closely track bulk $\delta^{13}C_{TOC}$ values. $\delta^{13}C$ values were measured for hopanes ranging in molecular mass from C_{27} to C_{32} (Table 2). For all hopanes reported in

Table 2
Mean carbon isotope compositions for individual extractable hopanes and hopenes measured by pico-CSIA (ratios measured in per mil versus VPDB), $C_{29}He$ = 29-norneohop-13(18)-ene, $C_{30}He$ = neohop-13(18)-ene, stdev = standard deviation, n = number of analyses.

Drill Core	Depth (m)	$C_{27}Tm$			$C_{27}\beta$			$C_{29}He$			$C_{29}\alpha\beta$			$C_{29}\beta\alpha$		
		$\delta^{13}C$ (‰)	stdev	n	$\delta^{13}C$ (‰)	stdev	n	$\delta^{13}C$ (‰)	stdev	n	$\delta^{13}C$ (‰)	stdev	n	$\delta^{13}C$ (‰)	stdev	n
Utkina Zavod	64.15	–22.73	0.19	2	–23.45	0.23	2	n.d.						–23.72		1
Utkina Zavod	71.67	−24.16	0.42	3	−24.11	0.19	3	−25.38		1						
Utkina Zavod	87	–23.54	0.35	2	–22.76	0.03	2	−25.60	0.11	3						
Utkina Zavod	111.6	–23.03	0.48	2	–22.95	0.13	2									
Utkina Zavod	124.6	–23.44	0.27	3	–23.37	0.31	3	−24.59	0.28	2	–23.94		1	–23.59	0.14	3
Utkina Zavod	153.5													−24.91	0.01	2
Lugovoe #13	41	−28.78	0.47	2	−28.22	0.05	2							−28.51	0.56	2
Lugovoe #13	47	–32.87	0.16	2	–32.20	0.19	2	–33.94	0.54	4	–32.61	0.43	3	–32.38	0.20	3
Lugovoe #13	71	–33.52	0.26	2	–32.99	0.15	2				−34.28	0.33	2	−34.12	0.37	2
Lugovoe #13	73	–32.75	0.63	2	–32.26	0.38	3				–33.8	0.33	2	–33.81	0.53	2
Gavrilov Yam −1	1860	–33.23	0.20	3	–32.32	0.21	3	−31.57	0.24	2	−34.02	0.65	2	−34.44		1
3628	226.5	−25.76	0.11	2	–23.97	0.18	2	−27.88	0.16	2	−26.34	0.07	2	−26.37	0.23	2
4592	~166	−30.19	0.30	2	−29.4	0.21	2				−30.78	0.65	2	−30.41	0.35	2

Drill Core	Depth (m)	$C_{30}\alpha\beta$			$C_{30}He$			$C_{30}\beta\alpha$			$C_{31}\alpha\beta S$			$C_{31}\alpha\beta R$		
		$\delta^{13}C$ (‰)	stdev	n	$\delta^{13}C$ (‰)	stdev	n	$\delta^{13}C$ (‰)	stdev	n	$\delta^{13}C$ (‰)	stdev	n	$\delta^{13}C$ (‰)	stdev	n
Utkina Zavod	64.15	−24.52	0.06	2	–23.50		1	–23.85	0.11	2				−24.64	0.07	2
Utkina Zavod	71.67	*–27.90*	*0.97*	*3*	−28.25		1							−25.16	0.08	3
Utkina Zavod	87	−24.11	0.18	3										−24.11	0.18	3
Utkina Zavod	111.6	−24.79	0.27	2										−24.64	0.26	2
Utkina Zavod	124.6	−24.74	0.05	2										−25.11	0.10	2
Utkina Zavod	153.5	−26.87	0.41	3										−26.75	0.8	3
Lugovoe #13	41	−29.05	0.35	2				−28.28	0.41	2				−30.14	0.83	2
Lugovoe #13	47	–32.60	0.06	3				–32.35	0.32	4				–32.90	0.09	3
Lugovoe #13	71	−34.29	0.29	3				–33.81	0.26	3	−35.34	0.24	2	−35.28	0.03	3
Lugovoe #13	73	–33.86	0.11	2				–33.65	0.33	2	−34.87	0.53	2	−34.64	0.19	3
Gavrilov Yam −1	1860	–32.98	0.01	2				–33.29	0.03	2				–33.68	0.27	2
3628	226.5	–27.69	0.35	2				−26.79		1	−28.32		1	−27.74		1
4592	~166	−30.56	0.24	2				−30.55	0.36	2	–32.29		1	−31.37	0.27	2

Drill Core	Depth (m)	$C_{31}\beta\alpha$			$C_{31}\beta\beta$			$C_{32}\alpha\beta R$		
		$\delta^{13}C$ (‰)	stdev	n	$\delta^{13}C$ (‰)	stdev	n	$\delta^{13}C$ (‰)	stdev	n
Utkina Zavod	64.15	−24.19	0.12	3	–23.47	0.13	2			
Utkina Zavod	71.67	−24.71	0.39	3	–23.77	0.38	3			
Utkina Zavod	87									
Utkina Zavod	111.6	–23.99		1						
Utkina Zavod	124.6	−24.41	0.20	3	−24.52		1			
Utkina Zavod	153.5									
Lugovoe #13	41	−28.82	0.05	2						
Lugovoe #13	47	–32.32	0.52	3						
Lugovoe #13	71	−34.78	0.11	3				−35.17	0.61	2
Lugovoe #13	73	−34.44	0.47	3				−34.66	0.04	2
Gavrilov Yam −1	1860	−34.62	0.35	2						
3628	226.5	−25.47	0.06	2						
4592	~166	−31.29	0.30	2						

Table 2, mean $\delta^{13}C_{hopane}$ differs from $\delta^{13}C_{TOC}$ in the host rocks by an average of only 1.3 ± 0.9‰ (Fig. 3a) for each sample. By contrast, the range of $\delta^{13}C_{hopane}$ found between differing drill-core locations and stratigraphic horizons is far larger, at 10.6‰. This holds for the two most abundant hopane constituents, 17α,21β-C_{30}(H) and 17α,21β,22R-C_{31}(H), which have an average $|\Delta\delta^{13}C_{hopane\ -\ TOC}|$ of 1.4 ± 0.7‰, even with a $\delta^{13}C_{hopane}$ range between samples for these compounds spanning 10.2‰ and 11.2‰, respectively.

The $\delta^{13}C_{values}$ of the C_{27}-C_{32} hopane series are more negative with increasing hopane carbon number, although the range for individual hopanes within any particular sample is fairly small (<4.5‰) considering that diverse groups of bacteria can biosynthesize hopanoids. The C_{27} hopanes have, on average, the most positive $\delta^{13}C$ values of the hopanes, followed by the C_{29}, and then the C_{30} hopanes. The C_{31} and C_{32} hopanes typically possess the most negative $\delta^{13}C$ signatures in our sample set.

The $\delta^{13}C_{hopane}$ values of the Utkina Zavod samples are close to $\delta^{13}C_{TOC}$ values but the relationship varies depending on the sample. Drill core 4592 $\delta^{13}C_{hopane}$ values are slightly more positive with respect to $\delta^{13}C_{TOC}$, while Gavrilov Yam drill core $\delta^{13}C_{hopane}$ values are all more negative with respect to $\delta^{13}C_{TOC}$. Lugovoe drill core $\delta^{13}C_{hopane}$ transitions from more negative with respect to $\delta^{13}C_{TOC}$ to more positive with respect to $\delta^{13}C_{TOC}$ moving stratigraphically upwards through the Redkino and Kotlin Regional horizons.

$\delta^{13}C$ values were measured for individual *n*-alkanes ranging from *n*-C_{17} to *n*-C_{29} (Table 3). The $\delta^{13}C_{n\text{-alkanes}}$ also closely match the $\delta^{13}C_{TOC}$ trend, although not as tightly as for the hopane compound series (Fig. 4). The $\Delta\delta^{13}C_{n\text{-alkane}\ -\ TOC}$ of the Lugovoe, 4592, and Gavrilov Yam drill-core samples all fall within 2.2‰ of $\delta^{13}C_{TOC}$. For the Utkina Zavod drill core, *n*-alkanes display a wider carbon isotope range, particularly among the *n*-C_{22} to *n*-C_{25} alkanes, which are as much as 6.6‰ more negative than $\delta^{13}C_{TOC}$. Overall, the *n*-alkanes from the Utkina Zavod drill core are on average more negative than $\delta^{13}C_{TOC}$ by 2.3‰, while the Lugove drill-core n-alkanes are on average 0.3‰ more positive than $\delta^{13}C_{TOC}$.

Despite the high hopane/sterane (Hop/Ster) abundance ratios for most samples, we were able to measure the $\delta^{13}C$ values of the C_{29}αααR sterane (stigmastane) in aliphatic fractions that exhibited a Hop/Ster ratio below 10 (Table 4). These were the Kotlin Regional Horizon samples, and the $\delta^{13}C$ values of the C_{29} sterane was within 0.7‰ of $\delta^{13}C_{TOC}$ values (Fig. 3b).

Isotopic compositions of the acyclic isoprenoids, pristane and phytane were also measured. Phytane $\delta^{13}C$ ranges from −1.8‰ to +0.2‰ relative to the $\delta^{13}C_{TOC}$ values for the Kotlin Regional Horizon samples. In contrast, phytane and pristane in the Lugovoe drill-core sample 13–71 (Redkino Regional Horizon) are very depleted in ^{13}C, with $\delta^{13}C$ values of −37.7‰ and −38.6‰, respectfully, and are more negative than $\delta^{13}C_{TOC}$ values by −4.6‰ and −5.5‰, respectively.

3.2. Tricyclic terpane ratios

The ratio of the C_{26}/C_{25} tricyclic terpanes (TT), measured from relative peak areas using MRM-GC–MS analysis, was used to help distinguish marine environments from fresh water/brackish settings. This parameter can be sensitive and informative about ancient aquatic salinity and can distinguish lacustrine from marine organic facies (Zumberge, 1987). It is especially useful for Precambrian OM since most biomarker ratios for distinguishing such salinity differences (for example, the presence or absence of 24-*n*-propylcholestanes from

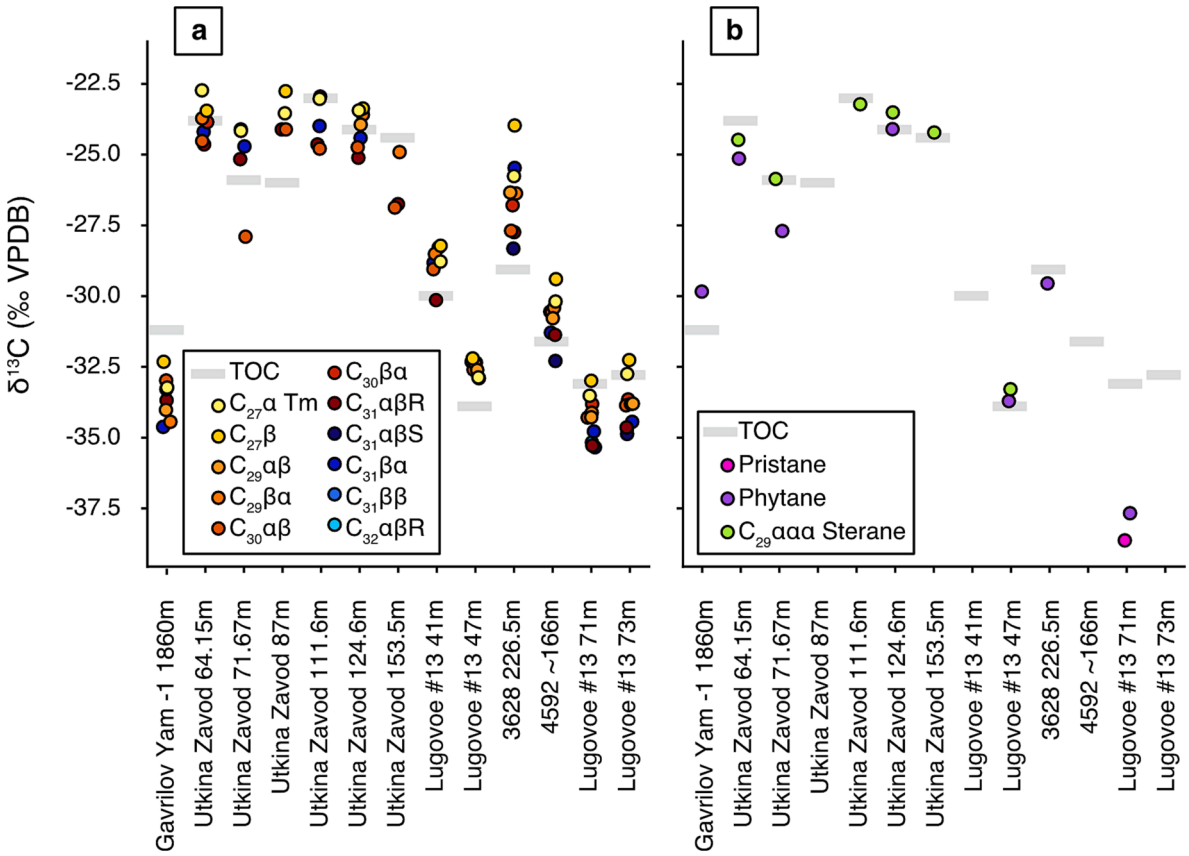

Fig. 3. (a) CSIA of individual hopanes and $\delta^{13}C_{TOC}$ for the late Ediacaran and Early Cambrian samples. (b) CSIA of pristane, phytane, C_{29} αααR sterane, and $\delta^{13}C_{TOC}$. The $\delta^{13}C_{org}$ values of C_{29} αααR sterane, mainly sourced by RuBisCO-CBB-utilizing green algae, tracks closely the $\delta^{13}C_{TOC}$ values. $\delta^{13}C_{org}$ values of pristane and phytane show a large negative offset compared to $\delta^{13}C_{TOC}$ values for samples Lugovoe 13–71 and 3628 226.5 m, but closely match $\delta^{13}C_{TOC}$ values for other samples. (For interpretation of the references to colour in this figure legend, the reader is referred to the web version of this article.)

Table 3
Mean carbon isotope ratios ($\delta^{13}C$) for individual extractable *n*-alkanes measured by pico-CSIA (ratios measured in per mil versus VPDB), stdev = standard deviation, n = number of analyses per sample.

Drill Core	Depth (m)	nC17			nC18			nC19			nC20			nC21		
		$\delta^{13}C$ (‰)	stdev	n	$\delta^{13}C$ (‰)	stdev	n	$\delta^{13}C$ (‰)	stdev	n	$\delta^{13}C$ (‰)	stdev	n	$\delta^{13}C$ (‰)	stdev	n
Utkina Zavod	64.15				−26.81	0.13	2	−26.49	0.11	2	−25.73	0.19	3	−25.6	0.12	2
Utkina Zavod	71.67				−28.39	0.69	3	−27.79	0.27	2	−27.3	0.03	2	−27.22	0.63	2
Utkina Zavod	87										−30.34	0.33	2	−29.42	0.18	2
Utkina Zavod	111.6										−25.54	0.58	2	−27	0.09	2
Utkina Zavod	124.6				−26.99	0.01	2	−26.03	0.41	2	−26.64	0.09	2	−26.66	0.15	3
Utkina Zavod	153.5															
Lugovoe #13	41							−30.23	0.41	2	−29.83	0.28	2	−29.84	0.2	2
Lugovoe #13	47				−33.07	0.14	3	−33.59	0.22	4	−33.68	0.21	4	−33.56	0.11	3
Lugovoe #13	71	−33.71		1	−33.15		1	−33.48	0.14	3	−34.10	0.24	3	−33.85	0.24	2
Lugovoe #13	73										−33.01	0.28	2	−32.68	0.67	2
Gavrilov Yam −1	1860				−30.4	0.27	2	−29.84	0.2	2	−30.13	0.16	2	−30.64	0.2	2
3628	226.5				−29.55	0.06	2	−28.9	0.05	2	−28.83	0.23	2	−28.76	0.05	2
4592	~166							−33.41	0.17	2	−32.31	0.13	3	−32.00	0.15	2

Drill Core	Depth (m)	nC22			nC23			nC24			nC25			nC26		
		$\delta^{13}C$ (‰)	stdev	n	$\delta^{13}C$ (‰)	stdev	n	$\delta^{13}C$ (‰)	stdev	n	$\delta^{13}C$ (‰)	stdev	n	$\delta^{13}C$ (‰)	stdev	n
Utkina Zavod	64.15	−26.13	0.28	2	−26.32	0.13	3	−26.79	0.05	2	−28.19	0.14	2	−23.63	0.21	2
Utkina Zavod	71.67	−27.79	0.03	2	−27.73	0.39	2	−27.6	0.14	2	−27.74	0.45	2	−25.22	0.31	2
Utkina Zavod	87	−30.78	0.55	2	−30.75	0.51	2	−31.79	0.18	2	−32.61	0.3	2	−29.25	0.27	2
Utkina Zavod	111.6	−28.06	0.66	2	−28.77	0.24	2	−26.54	0.17	2	−29.01	0.17	2	−23.36	0.16	2
Utkina Zavod	124.6	−27.07	0.1	2	−28.38	0.11	2	−28.36	0.17	2	−29.35	0.19	2	−26.27	0.4	2
Utkina Zavod	153.5															
Lugovoe #13	41	−30.24	0.11	2	−30.36	0.15	2	−31.08	0.01	2	−30.71	0.05	2	−30.65	0	2
Lugovoe #13	47	−33.36	0.11	3	−33.36	0.1	3	−33.01	0.04	3	−33.24	0.08	3	−33.12	0.2	4
Lugovoe #13	71	−33.21	0.43	2	−34.19	0.14	3	−32.07	0.73	2	−32.93	0.14	3	−31.92	0.40	3
Lugovoe #13	73	−32.6	0.16	2	−32.86	0.12	2	−30.56	0.01	2	−32.49	0.27	3	−31.07	0.11	3
Gavrilov Yam −1	1860	−31.19	0.19	2	−32.13	0.21	2	−32.74	0.21	2	−33.55	0.06	2	−33.08	0.14	2
3628	226.5	−28.85	0.12	2	−29.09	0.22	2	−29.1	0.03	2	−29.44	0.24	2	−27.76	0.11	2
4592	~166	−31.51	0.00	2	−31.58	0.17	3	−31.20	0.60	2	−30.91	0.27	2	−30.24	0.41	2

Drill Core	Depth (m)	nC27			nC28			nC29		
		$\delta^{13}C$ (‰)	stdev	n	$\delta^{13}C$ (‰)	stdev	n	$\delta^{13}C$ (‰)	stdev	n
Utkina Zavod	64.15	−24.64	0	2	−21.93	0.27	2			
Utkina Zavod	71.67	−26.94	0.61	2	−24.15	0.4	2			
Utkina Zavod	87	−29.35	0.31	2	−23.84	0.26	2	−23.75	0.11	2
Utkina Zavod	111.6	−24.9	0.12	2	−22.27	0.47	2			
Utkina Zavod	124.6	−26.65	0.03	2	−22.64	0.46	2	−23.95	0.33	3
Utkina Zavod	153.5									
Lugovoe #13	41	−29.97	0.43	2	−29.52	0.09	2	−29.1	0.36	2
Lugovoe #13	47	−32.99	0.1	3	−32.79	0.19	4			
Lugovoe #13	71	−32.56	0.25	3	−33.22	0.36	2			
Lugovoe #13	73	−31.51	0.31	3	−31.37	0.27	3			
Gavrilov Yam −1	1860	−31.73	0.21	2	−30.83	0.07	2	−31.48	0.09	2
3628	226.5	−27.35	0.01	2	−25.3	0.47	2	−27.33	0.12	2
4592	~166	−29.75	0.07	2	−29.92	0.38	2			

marine pelagophyte algae; Moldowan et al., 1990) are only applicable to Phanerozoic rocks and oils. A threshold value of > 1.2 usually indicates fresh water/brackish conditions, and high values from 1.4 and higher have been reported previously for freshwater, lacustrine source rocks (Zumberge, 1987; Korkmaz et al., 2022). The C_{26}/C_{25} TT abundance ratios for the Utkina Zavod drill-core samples are consistently elevated, ranging from 1.6 to 2.8 (Fig. 5, Table 1), whereas the remaining samples have lower values in the range of 0.4 to 1.5 (mean value = 1.0).

3.3. Iron Speciation

The Fe_{HR}/Fe_T ratios for Kotlin Regional Horizon samples range in value from 0.15 to 0.92 (Table 1). The majority of the Utkina Zavod and Volyn core samples of the Kotlin Regional Horizon have lower Fe_{HR}/Fe_T ratios, with several samples below 0.22, indicative of deposition under oxic water column conditions (Fig. 6). The Lugovoe samples from both the Kotlin and Redkino Regional horizons are all above 0.38, indicative of deposition under anoxic conditions (Poulton and Canfield, 2005). Fe_{py}/Fe_{HR} ratios are below 0.6 for all samples indicating that ferruginous, rather than euxinic, conditions were most common in during anoxic deposition (Poulton, 2021).

4. Discussion

4.1. $\delta^{13}C$ values of Lipid Biomarkers

The $\delta^{13}C$ values of individual alkane compounds and bulk sedimentary OM are controlled by the balance of a variety of biogenic inputs, as well as by local environmental conditions. Ancient epicontinental seaways were susceptible to changes in water circulation, redox, temperature, and sea level, which can all affect metabolic carbon isotopic fractionation relative to $\delta^{13}C_{DIC}$ and $\delta^{13}C_{TOC}$ (Pancost et al., 2013). As discussed in detail by Pehr et al. (2018), the sedimentary rocks from Baltica are exceptionally thermally well-preserved with multiple indicators (low $T_{max,}$ values consistent with immature hopane and sterane stereoisomer ratios) confirming their low thermal maturity as equivalent to a pre-oil window stage. Thermal maturation effects on $\delta^{13}C$ values due to cracking of biomolecules are therefore minimal. Significant overprinting from migrated OM from petroleum fluids can also be ruled out based on the immature biomarker stereoisomer

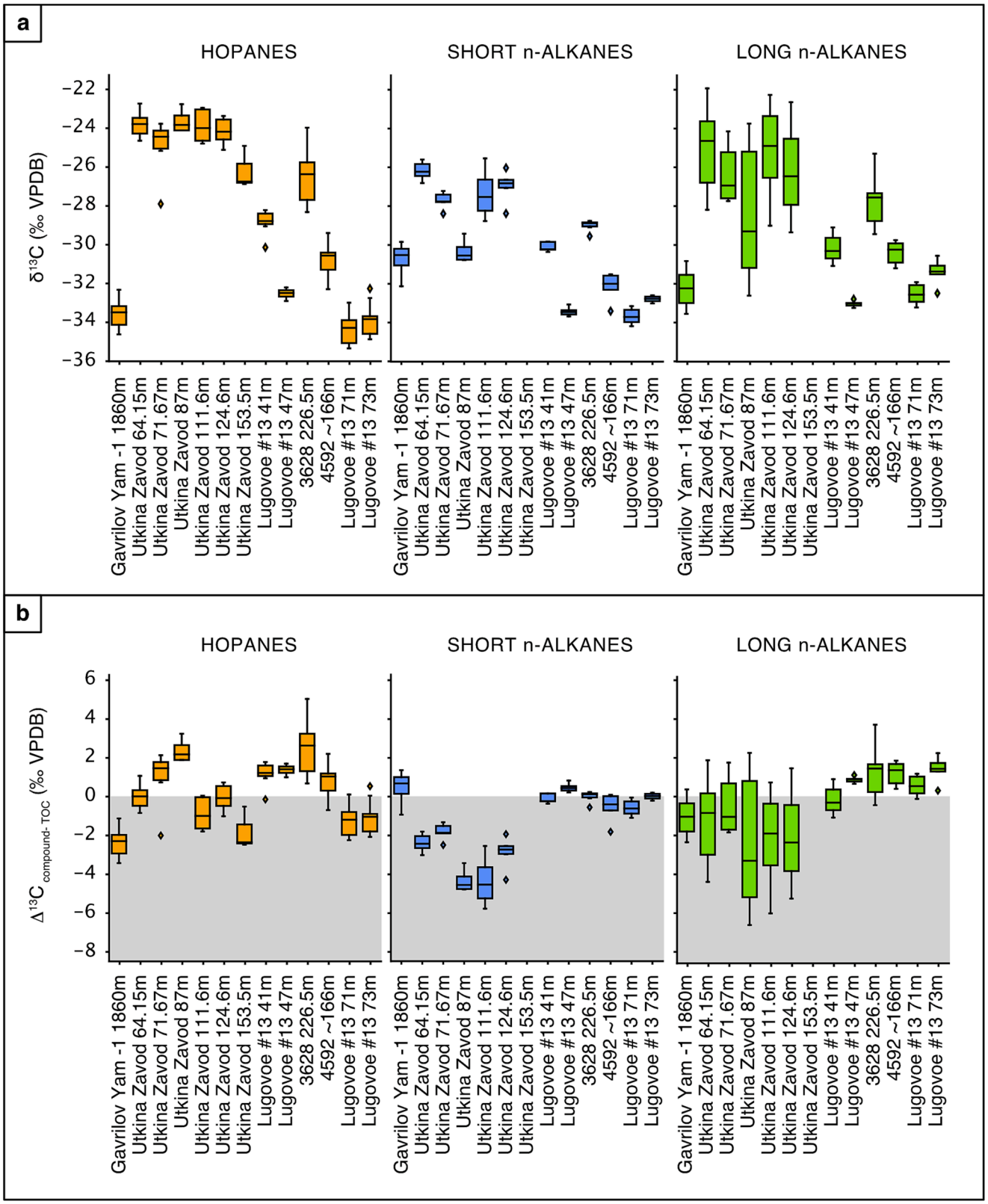

Fig. 4. (a) Box plots of CSIA of hopanes, short-chain *n*-alkanes (range shown for *n*-C_{17} to *n*-C_{21}), and long-chain *n*-alkanes (range shown for *n*-C_{22} to *n*-C_{29}). Mean $\delta^{13}C_{hopane}$ values vary by 10.6‰, mean $\delta^{13}C_{short\ n\text{-}alkanes}$ values vary by 7.5‰, and mean $\delta^{13}C_{long\ n\text{-}alkanes}$ values vary by 7.7‰ from sample to sample. (b) Box plots of CSIA relative to $\delta^{13}C_{TOC}$ values for hopanes, short-chain *n*-alkanes (*n*-C_{17} to *n*-C_{21}), and long-chain *n*-alkanes (*n*-C_{22} to *n*-C_{29}).

Table 4
Mean carbon isotope compositions for extracted pristane (Pr), phytane (Ph), and C_{29} αααR sterane, measured by pico-CSIA (ratios measured in per mil versus VPDB) and carbon isotope difference between *n*-alkanes and acyclic isoprenoids from the same samples, including pristane (Pr), phytane (Ph), nC_{17} and nC_{18}; stdev = standard deviation, n = number of repeat CSIA analyses per sample.

Drill Core	Depth (m)	Pr			Ph			C_{29} Ster αααR			$\delta^{13}C_{nC17\text{-}Pr.}$	$\delta^{13}C_{nC18\text{-}Ph.}$
		$\delta^{13}C$ (‰)	stdev	n	$\delta^{13}C$ (‰)	stdev	n	$\delta^{13}C$ (‰)	stdev	n	(‰)	(‰)
Utkina Zavod	64.15				−25.14	0.13	2	−24.48		1		−1.67
Utkina Zavod	71.67				−27.7	0.31	3	−25.86	1.36	2		−0.69
Utkina Zavod	87											
Utkina Zavod	111.6							−23.22	0.26	2		
Utkina Zavod	124.6				−24.1	0.08	3	−23.51	0.16	2		−2.89
Utkina Zavod	153.5							−24.22	0.24	2		
Lugovoe #13	41											
Lugovoe #13	47				−33.71	0.18	2	−33.29	0.17	3		0.64
Lugovoe #13	71	−38.63		1	−37.67		1				4.92	4.52
Lugovoe #13	73											
Gavrilov Yam −1	1860				−29.84	0.29	2					−0.56
3628	226.5				−29.55	0.16	2					0.00
4592	~166											

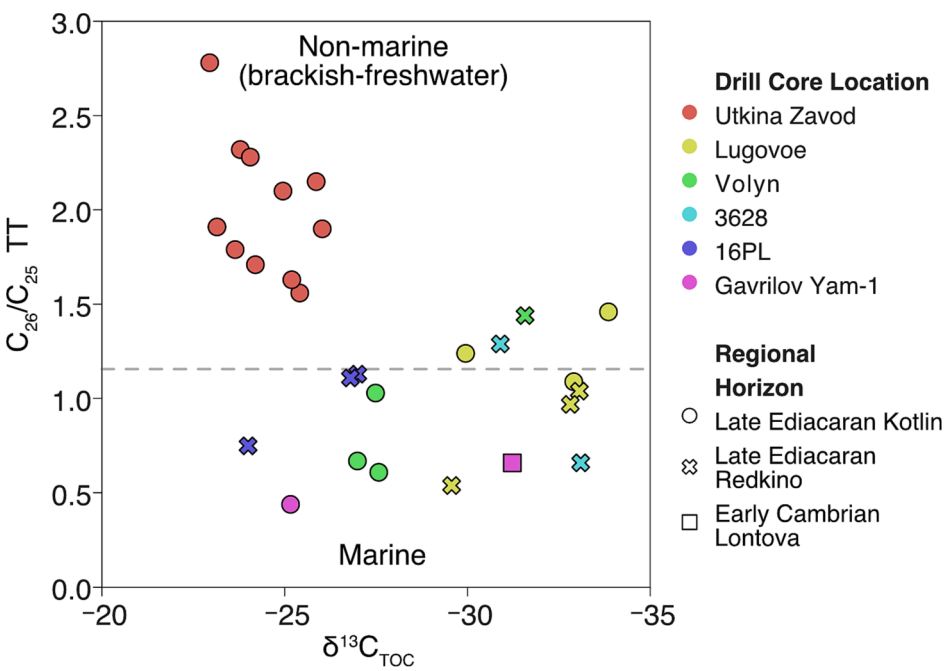

Fig. 5. Bulk organic carbon isotope values ($\delta^{13}C_{TOC}$) versus the ratio of C_{26}/C_{25} tricyclic terpanes (TT); C_{26}/C_{25} TT > 1.2 usually indicates lower-salinity, aquatic environments, either freshwater or brackish; C_{26}/C_{25} TT < 1.2 (dashed line) is typically indicative of normal marine conditions. Here, values > 1.2 are likely indicative of marginal marine/estuarine setting with brackish waters. Notably, the Utkina Zavod drill-core sediments from the Kotlin Regional Horizon all fall within the non-marine field.

patterns found, and from the self-consistency check provided from parallel analysis of kerogen-bound hydrocarbons (Pehr et al., 2018).

Hopanes, the most abundant compounds in the aliphatic fractions, have $\delta^{13}C$ values that closely track $\delta^{13}C_{TOC}$ values. Derived from hopanoids, these cell membrane lipids are synthesized by a wide variety of bacterial groups (Rohmer et al., 1984; Pearson et al., 2007). Given their high abundance (Fig. 2), the ancient hopanes were likely derived from both bacterial primary producers and heterotrophs. Across all samples, most isotope values for hopane compounds are fairly close (±2‰) to the $\delta^{13}C_{TOC}$ values. However, delta values for individual hopanes in any particular sample can differ from TOC by up to 4‰, which likely reflects the production-weighted average from multiple bacterial lipid sources. The slightly more positive carbon isotope ratios for the lower carbon number hopanes, particularly C_{27} compounds, may be due to a greater degree of diagenetic reworking of these compounds within the water column and sediments. C_{27} hopanes are derived from complete side-chain cleavage of C_{30} and/or C_{35} biohopanoid precursors and hence are the most altered hopane compounds within the series.

Carbon isotope compositions of *n*-alkanes are either more negative (particularly for some samples from the Utkina Zavod drill core) or close to $\delta^{13}C_{TOC}$. The offset between free alkanes and bulk TOC (mainly composed of kerogen) could, in theory, reflect the isotopic differences between lipids and melanoidin-like organic geopolymers containing significant contributions from non-lipid biochemicals (carbohydrates or proteins).

Sterane distributions are more diagnostic of specific biological sources than hopanes. A dominance of C_{29} steranes, derived from C_{29} sterol precursors, represents contributions by green algae and plants (Grantham and Wakefield, 1988; Schwark and Empt, 2006; Kodner et al., 2008; Love et al., 2009). Prior to the appearance of terrestrial plants in the Paleozoic, a C_{29} sterane (stigmastane) dominance generally indicates high green algal inputs (Grosjean et al., 2009; Love et al, 2009). Green algae are primary producers, which use RuBisCO-CBB for autotrophic carbon fixation, a pathway that yields biomass fractionated by up to ca. −29‰ from the $\delta^{13}C$ values of dissolved CO_2 (Roeske and O'Leary, 1984; Hayes, 2001; Scott et al., 2004; Pearson, 2010; Carvalho and Eyre, 2011).

For Ediacaran OM preserved in ancient sedimentary rocks, extractable alkane fractions typically have very similar bulk $\delta^{13}C$ signatures, within ~ 1‰ (Grosjean et al., 2009), relative to $\delta^{13}C_{TOC}$ values. The

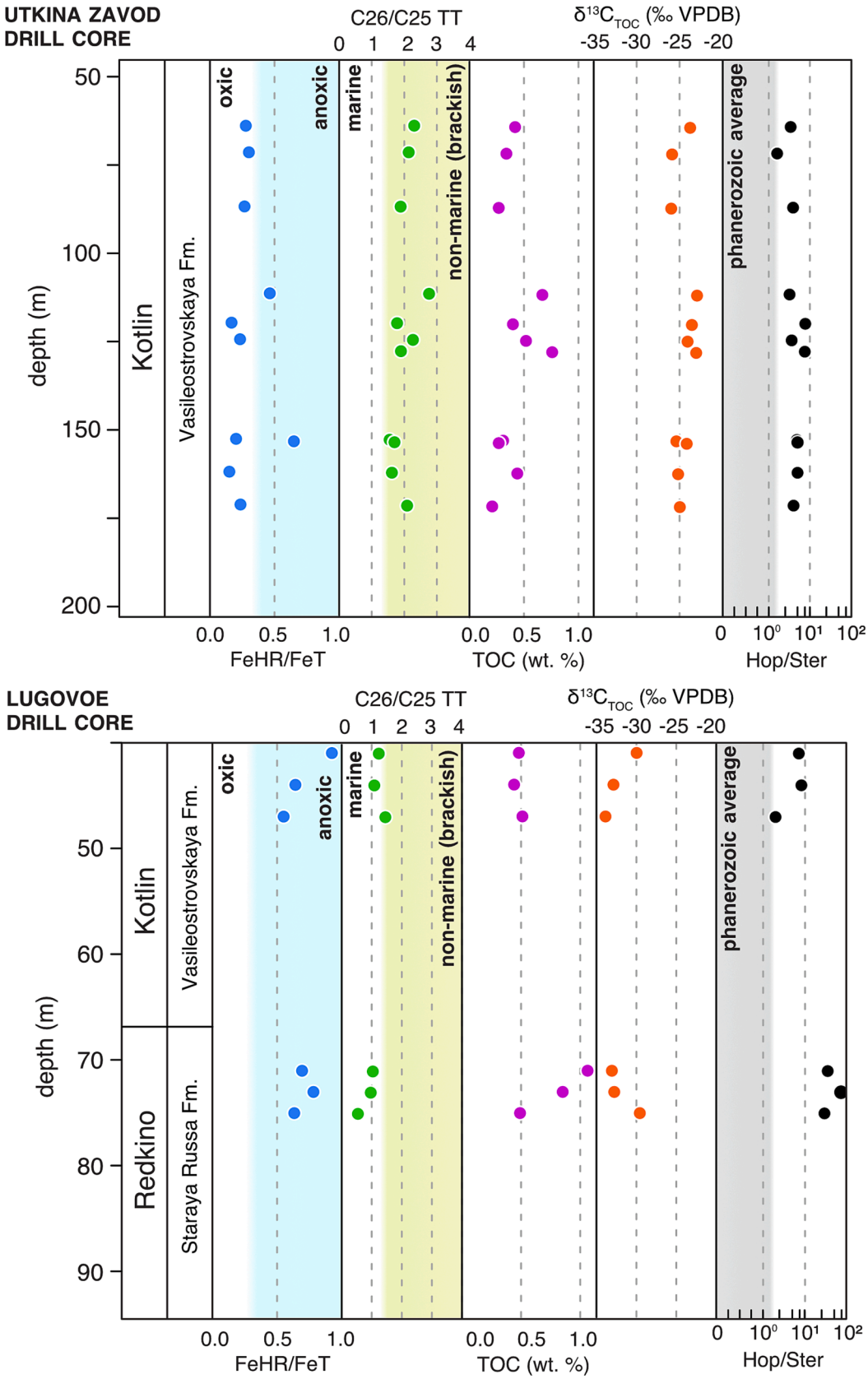

Fig. 6. Stratigraphic trends for inorganic and organic geochemical proxies measured for sediments from the Utkina Zavod and Lugovoe drill cores. C_{26}/C_{25} TT (tricyclic terpanes), FeHR/FeT, δ^{13}CTOC, TOC, and Hop/Ster values are given in Table 1. The threshold value for C_{26}/C_{25} TT is ~ 1.2 to distinguish low-salinity lacustrine or marginal marine waters (>1.2) from marine waters (≤1.2).

most ^{13}C-depleted ancient and modern alkane compounds produced by marine autotrophs using RuBisCO-CBB for carbon fixation are around −36‰, and is typically associated with times of high atmospheric pCO_2 (Pagani et al., 2005), which maximizes biological carbon isotope fractionations by autotrophs (Hayes, 1993). However, it is common to observe less than the maximum possible fractionation value, due to elevated growth rates associated with high nutrients or other environmental factors. The $\delta^{13}C_{C29sterane}$ values for our samples range from –23.22‰ to –33.29‰ and closely align with the corresponding $\delta^{13}C_{TOC}$ and $\delta^{13}C_{hopane}$ values. The most negative $\delta^{13}C_{C29sterane}$ value of –33.29‰ still falls within the predicted ^{13}C-depleted range for lipids derived from green algae. Strikingly similar δ^{13}C values for C_{29} ααα R sterane and the most abundant (C_{27}-C_{32}) hopanes suggest that the major bacterial source organisms included RuBisCO-CBB-utilizing photoautotrophs, such as cyanobacteria, as well as bacterial heterotrophs consuming primary biomass.

4.2. Local Environmental Effects on $\delta^{13}C_{TOC}$

Organics in the Utkina Zavod drill-core samples are enriched by ~ 10‰ compared to other samples of late Ediacaran – Early Cambrian including other localities in Baltica used in this study (Table 1), and for sediments and oils from South Oman, Siberia, Australia, and South China (Grosjean et al., 2009; Kelly et al., 2011; Lan et al., 2012; Lee et al., 2013; Pagès et al., 2016; Wang et al., 2019; Roussel et al., 2020). This enrichment is observed in both the bulk TOC and individual compounds. CSIA data reveal the Kotlin Regional Horizon ^{13}C-enrichment is captured across a variety of major lipid compound classes, including the hopanes, *n*-alkanes, phytane, and C_{29} ααα R sterane. The large magnitude of this ^{13}C-enrichment, which is unusual for Ediacaran marine samples, points to unusual environmental conditions during deposition of the Kotlin Regional Stage strata at the Utkina Zavod drill-core location. In contrast to other depositional sites in Baltica, the data are suggestive of a non-marine and/or highly restricted aquatic setting.

The ~ 10‰ difference between the Utkina Zavod and Lugovoe drill cores, which are < 100 km apart in the Saint Petersburg area of Russia, could reflect the δ^{13}C composition of the local DIC pool or metabolic fractionation potentially related to nutrient-fueled growth rates or productivity- or circulation-linked differences in dissolved CO_2 concentrations (Fogel et al., 1992; Popp et al., 1998). Notably, lipid compounds from phototrophs carry the enrichment. Thus, we can rule out other factors that influence isotope abundances in bulk sedimentary organic matter, including heterotrophic reworking, enhanced preservation of protein and carbohydrate residues as melanoidin-like geopolymers, or shifts in the microbial communities.

Diminished fractionation by photoautotrophs can result from several mechanisms. Low $CO_{2(aq)}$ concentrations limit the flux of carbon supplied across cell membranes by diffusion, which limits expression of enzymatic isotope fractionation during carbon fixation. Low concentrations and associated carbon limitation can further trigger carbon-concentration mechanisms (CCM), including active bicarbonate uptake (Badger and Price, 2003; Reinfelder, 2011). These active carbon transport mechanisms yield biomass that is significantly enriched in ^{13}C (Hayes, 1993; Smith et al., 1999). In modern marine waters, $CO_{2(aq)}$ concentrations represent a balance between carbon uptake by photosynthesis with that supplied by upwelling and equilibration with the atmosphere, and potential carbonate equilibria shifts tied to pH and water temperatures (Freeman, 2001). Atmospheric CO_2 concentrations were likely high in the late Ediacaran – Early Cambrian (Kanzaki and Murakami, 2018; Mills et al., 2019), and, more importantly, as a global feature they would not differ by locality, so this option seems unlikely. Variations in nutrient supply and ocean circulation or upwelling could have varied by locality.

Diminished fractionation can also result from increased carbon demand due to elevated phytoplankton growth rates spurred by high nutrient availability. Elevated productivity is often associated with enhanced OM burial efficiency due to decreased oxygen exposure times (Hartnett et al., 1998). Yet, craton-scale low nutrient, oligotrophic conditions have been inferred for Baltica during the late Ediacaran to Early Cambrian (Pehr et al., 2018). This inference is based on the absence of evidence for enhanced carbon burial, including consistently low TOC content (mostly < 0.5 wt%), low Hydrogen Index values for TOC, and biomarkers signifying bacterial input dominance over eukaryotes.

It is conceivable that the absence of evidence for enhanced carbon burial reflects more efficient heterotrophic respiration. If so, substantial biomass from elevated productivity was largely not preserved in the sedimentary rock record. This is possible under the mainly oxic (based on Fe speciation, Fig. 6) and oligotrophic conditions, which implies that well ventilated conditions persisted in the coastal waters at the Utkina Zavod drill-core location during the Kotlin Regional Stage (Pehr et al., 2018). However, there is no geochemical evidence for enhanced carbon remineralization such as accumulation of pyrite or Fe- and Mn-rich carbonates, and geochemical proxies for reducing water-column redox conditions in the sample localities. Combined, this evidence points to lower rates of primary biomass production due to limited nutrient supplies.

The C_{26}/C_{25} tricyclic terpane (TT) ratio, which tracks environmental conditions during deposition, clearly differentiates between the Utkina Zavod and Lugovoe drill-core samples of the Kotlin Regional Horizon. The ratio of C_{26}/C_{25} TT correlates with the salinity in the depositional setting (Zumberge, 1987). C_{26}/C_{25} TT values at or below ~ 1.0 are associated with marine conditions, whereas values greater than or equal to ~ 1.2 are typically associated with brackish or freshwater conditions (Zumberge, 1987; Grande et al., 1993). Intermediate values of 1.0–1.2 are equivocal. The Utkina Zavod drill-core samples (C_{26}/C_{25} TT ranges 1.6 to 2.8, mean = 2.0) all fall within the range of brackish-freshwater conditions. In contrast, the Lugovoe drill-core samples have values that range from 0.5 to 1.5 (mean = 1.1), close to normal marine conditions.

The tricyclic terpane ratios suggest that sediments from the Utkina Zavod drill-core were deposited under lower salinities, typical of a coastal setting. They also indicate the Lugovoe sediments, sitting < 100 km north towards the craton margin, were deposited in a less restricted marine setting. The Lugovoe drill-core biomarker distributions also have noticeably higher ratios of C_{31}/C_{30} hopanes than those for the Utkina Zavod drill-core rocks. This difference is consistent with iron speciation data that indicate that the Lugovoe location hosted more reducing water-column conditions during the Kotlin Regional Stage (Figs. 1 and 6). A low salinity coastal setting at Utkina Zavod drill core is consistent with the environmental conditions inferred for the Kotlin Regional Stage in Estonia, located more than 150 km west-southwest of the Utkina Zavod drill core. In Estonia, a fresh-brackish aquatic setting with warm and humid climatic conditions was suggested based on a common presence of diagenetic siderite, lack of pyrite and glauconite, and low boron content in the clay fraction of fine-grained siliciclastic sediments (Pirrus, 1992; Mens and Pirrus, 1997). Freshwater conditions on the western side of the East European craton during the Ediacaran were also described based on the occurrence of pedogenic siderites (Bojanowski et al., 2019).

Shallow coastal, deltaic, and estuarine environments are the mixing zone of marine and fresh waters, and pH and temperature are more variable than in open-marine environments. Freshwater feeding into the coastal waters could have had a higher pH and higher alkalinity, that varied depending on the water provenance (Krishna et al., 2018). The proportion of $CO_{2(aq)}$ versus both bicarbonate and carbonate within the DIC pool decreases with higher pH (Zhang et al., 1995), resulting in a potential $CO_{2(aq)}$ limitation. We suggest alkaline riverine water input to the brackish coastal waters led to higher pH and/or alkalinity, resulting in $CO_{2(aq)}$ limitation and enhanced utilization of CCMs and bicarbonate uptake by phytoplankton. These processes likely contributed to the ^{13}C-enriched composition of TOC and individual lipid biomarkers during

deposition of the Kotlin Regional Horizon at the Utkina Zavod drill-core location.

In modern esutaries, the $\delta^{13}C$ values of DIC are typically more negative than marine values, due to the remineralization of organic carbon from plants and soil (Fogel et al., 1992; Boschker et al., 2005). However, terrestrial inputs of organic carbon would have been very low in the late Ediacaran to the Early Cambrian, due to the absence of land plants. It is possible that seawater input of DIC derived from carbonate weathering may have contributed more positive $\delta^{13}C_{DIC}$ values to the coastal environment (Kump and Arthur, 1999; Kump et al., 1999), although it seems unlikely that the aqueous $\delta^{13}C_{DIC}$ shifted by as much as ~ 10‰ to solely drive the change in the $\delta^{13}C_{TOC}$. Further, pre-late Ediacaran (Cryogenian and Tonian) sedimentary successions are predominantly siliciclastic on Baltica and so they could not have been a significant source of inorganic carbon input.

There has been some emerging evidence for localized nearshore DIC gradients in late Ediacaran marine margins, resulting in ^{13}C-enriched sedimentary OM and carbonates. This is supported by gradients in $\delta^{13}C_{carb}$ of carbonates deposited in basinal and proximal ramp settings, for late Ediacaran marine rocks in Namibia (Wood et al., 2015). More positive values of $\delta^{13}C_{carb}$ were associated with proximal (inner ramp) depositional settings. The underlying cause of this phenomenon is not well understood and the magnitude of the local isotopic gradients does not typically exceed ~ 3-4‰ (Wood et al., 2015). Thus, these gradients are significantly smaller in magnitude than the > 10‰ differences in $\delta^{13}C$ values of individual lipids and bulk OM between drill-core locations. Local and regional dissolved carbon isotope gradients do not explain the full ~ 10‰ enrichment for the Kotlin Regional Horizon in bulk TOC and individual lipids in Utkina Zavod drill core versus Ediacaran seawater-sourced sedimentary OM.

The anomalous and consistently ^{13}C-enriched signature of the Kotlin Regional Horizon succession in Utkina Zavod drill-core and the absence of marine gradients in productivity, nutrients, or $\delta^{13}C_{DIC}$ collectively suggest fundamentally different depositional environments for the drill-core locations. We suggest the Utkina Zavod section was deposited in a brackish epicontinental setting. This is supported by elevated C_{26}/C_{25} TT values from 1.6 to 2.8 (Fig. 5, Table 1) that are consistent with low (fresh to brackish) coastal salinity. Elevated 2-methylhopane index values of 5.1 to 9.9% for samples from Utkina Zavod drill core (Pehr et al., 2018) are also consistent with a low-salinity, coastal setting, and may signify cyanobacterial and/or proteobacterial sources for the hopanes and 2-methylhopanes (Naafs et al., 2022), along with bacterial heterotrophs, in these samples. Geochemical evidence suggests the brackish coastal waters transitioned into normal-marine salinity conditions further offshore at the Lugovoe drill-core location. Such environmental differences may ultimately be tied to global eustatic sea level, climatic, and ocean–atmosphere redox changes, which occurred during the late Ediacaran (Li et al., 2019) and likely shaped local salinity conditions in marginal marine settings.

4.3. Investigating Evidence for Inverse Isotopic Ordering

Samples from the Lugovoe, 4592, and 3628 drill cores all display an unusual isotopic enrichment of the *n*-alkanes relative to bulk TOC, a characteristic which has been described previously as an "inverse carbon isotopic ordering" because lipids are depleted in ^{13}C relative to biomass for most modern organisms (Hayes 2001) (Fig. 4.). Among these samples, those from the Redkino Regional Horizon in the Lugovoe drill core also show a strong positive enrichment between nC_{17} and nC_{18} alkanes vs. pristane and phytane (Table 4). Similar trends are reported for other Neoproterozoic samples (Logan et al., 1995, 1997) and are considered a common characteristic in late Precambrian marine basins. Sample Lugovoe #13 (collected at 71 m depth), has a $\delta^{13}C_{nC17\text{-}Pr}$ value of + 4.92‰ and a $\delta^{13}C_{nC18\text{-}Ph}$ value of + 4.52‰, which are suggestive of this inverse carbon isotopic ordering. The remaining samples from the Utkina Zavod and Lugovoe drill cores for which phytane isotopic compositions were measurable, feature much less positive $\delta^{13}C_{nC18\text{-}Ph}$ values, which ranged from −2.89 to + 0.64‰ and which are closer to more typical Phanerozoic carbon isotope ordering.

Previous explanations for isotopic enrichment in *n*-alkanes included: (1) intense heterotrophic reworking of slowly sinking OM (in the absence of animals that repackage OM to fecal pellets) in a redox-stratified ocean (Logan et al., 1995, 1997), or (2) a significant difference in carbon isotope fractionation between bacterial and eukaryotic primary producers (Close et al., 2011). Both arguments assume preferential preservation of certain compounds within kerogen, which generally accounts for most of the bulk TOC in ancient rocks.

For the Redkino Regional Horizon samples from Lugovoe drill core in our dataset, there is a third potential explanation. Pristane and phytane are commonly derived from the phytol side chain of certain chlorophylls made by photosynthetic organisms, particularly cyanobacteria and algae (Rontani and Volkman, 2005). However, Lugovoe #13 sample (collected at 71 m depth) has a $\delta^{13}C_{phytane}$ value of −37.7‰ and a $\delta^{13}C_{pristane}$ value of −38.6‰, well below values typical for RuBisCO-CBB-utilizing phototrophs. Such low values (ca. −39‰) indicate the acyclic isoprenoids derived in part from microorganisms involved in methane cycling (Freeman et al., 1990) mixed with input from chlorophylls with a phytol side chain. Additionally, methanogenic and methanotrophic archaea synthesizing archaeol/hydroxy-archaeols have been proposed as a possible source for phytane (Koga et al., 1993; Koga et al., 1998; Wakeham et al., 2003), and could have feasibly contributed to pristane from diagenetic modification of phytane.

Thus, the > 4‰ offset for $\Delta\delta^{13}C_{nC18\text{-}Ph}$ could reasonably be explained by unusually ^{13}C-depleted phytane from an appreciable archaeal source, rather than ^{13}C-enrichment of *n*-alkanes due to intense heterotrophy. Archaeal lipid inputs is supported by CSIA data reported for pristane and phytane in Ediacaran-Cambrian oils from Siberia. These oils yielded similar $\delta^{13}C_{pristane}$ and $\delta^{13}C_{phytane}$ values that were as low as ca. −44‰ and about half of the samples had ^{13}C-depletion of $\delta^{13}C_{pristane}$ and $\delta^{13}C_{phytane}$ of −1 to −8‰ compared with nC_{17} and nC_{18} alkanes. (Kelly et al., 2011). The interiors of the deep oceans were likely not fully oxygenated through most of the Paleozoic Era (Stolper and Bucholz, 2019), which would have favored methanogenesis and sustained a vigorous methane cycle in the water column and in shallow sediments in the Precambrian and Early Paleozoic oceans (Rohrssen et al., 2013).

Our CSIA measurements were not limited to *n*-alkane and acyclic isoprenoid carbon isotopes. With the enhanced sensitivity of pico-CSIA, we were able to measure $\delta^{13}C$ signatures for the C_{27}-C_{32} hopanes and the most abundant C_{29} sterane (αααR). This allowed us to investigate the possible origins of these important and diagnostic markers of biological sources.

Hop/Ster ratios can be used as convenient estimates of bacterial versus eukaryotic source contributions to preserved sedimentary OM. Environments with high rates of heterotrophy may preserve elevated Hop/Ster ratios due to an abundance of hopanoid-producing heterotrophic bacteria. While the Lugovoe, 4592, and 3628 drill cores have high Hop/Ster ratios (>1), spanning from 2 to 119, there is no corresponding significant change in $\Delta\delta^{13}C_{n\text{-alkane - TOC}}$. Biomass from heterotrophic bacteria is also typically enriched in ^{13}C relative to their food source by ~ 1‰ (DeNiro and Epstein, 1978; Hullar et al., 1996). Previous models of inverse carbon isotopic ordering have assumed a significant difference in carbon isotope composition between photosynthetic bacteria and eukaryotic biomass of, at a minimum, 4‰ (Close et al., 2011). For the one Lugovoe drill-core sample (collected at 47 m depth) with a measurable $\delta^{13}C_{C29sterane}$ value, the average $\delta^{13}C_{hopane}$ value is only ~ 0.6‰ more positive relative to $\delta^{13}C_{C29sterane}$. This is much less than the 4‰ biogenic offset thought to be needed to produce a ^{13}C-enrichment in the n-alkanes. This is also in line with our other sterane measurements for the Utkina Zavod drill-core samples, which yield a mean and maximum $\Delta\delta^{13}C_{hopane\ -\ C29sterane}$ of 0.8‰ and 2.7‰, respectively.

Overall, this evidence suggests the late Ediacaran rocks reported here

do not simply conform to the typically prescribed Precambrian inverse carbon isotopic ordering of linear alkanes versus acyclic isoprenoids. Further, we found no significant difference in the average carbon isotope abundances measured for polycyclic triterpanes from bacterial producers and consumers versus the main eukaryotic (green algal) primary producers in the rock sample with measurable $\delta^{13}C_{C29sterane}$ and $\delta^{13}C_{hopanes}$ (mean = 0.6‰). The combined evidence points to the abundant bacterial signal being at least partially sourced from phototrophic bacteria, particularly RuBisCO-CBB-utilizing bacteria, alongside a significant contribution from heterotrophic bacteria.

Importantly, multiple source contributions to *n*-alkanes and to phytane (including from archaeal sources as well as from chlorophylls), complicate the carbon isotopic systematics. Such source variations were likely tied to changing paleoenvironmental redox that can mute or exaggerate $\delta^{13}C$ differences between compounds. Indeed, the magnitude of Ediacaran inverse/normal carbon isotopic ordering of branched versus linear alkanes, normally attributed to a preferential heterotrophic reworking of *n*-alkanes or a significant difference in $\delta^{13}C$ between algal and bacterial lipids, was likely influenced by multiple environmental and ecological factors. Future studies utilizing the improved pico-CSIA method on ancient sedimentary rocks and oils will help shed new light on the secular patterns and the carbon isotopic systematics for a suite of ancient lipid compounds.

5. Conclusions

During the late Ediacaran, Baltica was covered by shallow, epicontinental seas extending from the foreland basins developed along the southwestern, eastern, and northeastern margins. This contributed to oligotrophic conditions and a high regional heterogeneity in marine environments, including brackish coastal waters. The lipid biomarker and stable carbon isotopic characteristics of the strata from the Kotlin Regional Horizon from the Utkina Zavod drill core suggest that these sediments were deposited in a fresh to brackish water-column coastal setting rather than in an open-marine environment. $\delta^{13}C$ values for bulk organics and individual compounds from the Utkina Zavod drill core are more positive than typical Ediacaran marine settings (range −26.0 to –23.0‰) and generally track each other, slightly offset by < 2‰. The $\delta^{13}C_{TOC}$ values matched those for pristane, phytane, and C_{29} αααR sterane, which are typically derived from photoautotrophs. The low salinity coastal waters that prevailed during deposition of the Kotlin Regional Horizon strata at the Utkina Zavod drill-core location may have sustained high pH and/or elevated alkalinity of carbonate and bicarbonate from riverine input. This could have resulted in localized dissolved $CO_{2(aq)}$ limitation that promoted carbon-concentration mechanisms or active bicarbonate uptake by photoautotrophs, explaining the consistently ^{13}C-enriched signature found for lipids and bulk TOC in the Kotlin Regional Horizon sediments.

By contrast, the sedimentary OM in sediments from the Kotlin and Redkino Regional horizons from the Lugovoe drill core exhibit isotope signatures that are more typical of Ediacaran marine settings ($\delta\ ^{13}C_{TOC}$ ranging from –33.9 to −30.0‰). Very high ratios of Hop/Ster in these sediments, combined with similar $\delta^{13}C$ values for C_{29} sterane and individual hopanes, strongly indicate that the major source biota were photoautotrophic bacteria utilizing RuBisCO-CBB and heterotrophic bacteria, with a lesser contribution from green algae. The most depleted $\delta^{13}C$ signatures for lipids are found in a Lugovoe drill-core sample from the Redkino Regional Horizon. $\delta^{13}C$ values for pristane and phytane are significantly depleted to −39‰, suggesting a partial contribution of acyclic isoprenoids from archaea involved in methane cycling.

Declaration of Competing Interest

The authors declare that they have no known competing financial interests or personal relationships that could have appeared to influence the work reported in this paper.

Data availability

Data are in the tables in the manuscript attachment

Acknowledgements

We dedicate this paper to the late Marilyn Fogel, who pioneered methods in stable isotope geochemistry and organic geochemistry. Marilyn's dedication to science and the mentorship of young scientists over many years was recognized and appreciated by many individuals within the geochemistry community. G.D.L. acknowledges a NASA Exobiology award (grant number 80NSSC18K1085) for funding this research. A.B. thanks Petroleum Foundation of the American Chemical Society (grant number 624840ND2). We also thank the two anonymous reviewers for their helpful comments.

References

Baczynski, A.A., Polissar, P.J., Juchelka, D., Schwieters, J., Hilkert, A., Summons, R.E., Freeman, K.H., 2018. Picomolar-scale compound-specific isotope analyses. Rapid Communications in Mass Spectrometry 32, 730–738.
Badger, M.R., Price, G.D., 2003. CO2 concentrating mechanisms in cyanobacteria: molecular components, their diversity and evolution. Journal of Experimental Botany 54, 609–622.
Bobrovskiy, I., Hope, J.M., Golubkova, E., Brocks, J.J., 2020. Food sources for the Ediacara biota communities. Nature Communications 11, 1261.
Bojanowski, M.J., Goryl, M., Kremer, B., Marciniak-Maliszewska, B., Marynowski, L., Środoń, J., 2019. Pedogenic siderites fossilizing Ediacaran soil microorganisms on the Baltica paleocontinent. Geology 48, 62–66.
Boschker, H.T.S., Kromkamp, J.C., Middelburg, J.J., 2005. Biomarker and carbon isotopic constraints on bacterial and algal community structure and functioning in a turbid, tidal estuary. Limnology and Oceanography 50, 70–80.
Brocks, J.J., Jarrett, A.J.M., Sirantoine, E., Hallmann, C., Hoshino, Y., Liyanage, T., 2017. The rise of algae in Cryogenian oceans and the emergence of animals. Nature 548, 578–581.
Canfield, D.E., Raiswell, R., Westrich, J.T., Reaves, C.M., Berner, R.A., 1986. The use of chromium reduction in the analysis of reduced inorganic sulfur in sediments and shales. Chemical Geology 54, 149–155.
Canfield, D.E., Raiswell, R., Bottrell, S.H., 1992. The reactivity of sedimentary iron minerals toward sulfide. American Journal of Science 292, 659–683.
Carvalho, M., Eyre, B., 2011. Carbon stable isotope discrimination during respiration in three seaweed species. Marine Ecology Progress Series 437, 41–49.
Close, H.G., Bovee, R., Pearson, A., 2011. Inverse carbon isotope patterns of lipids and kerogen record heterogeneous primary biomass. Geobiology 9, 250–265.
Coplen, T.B., Brand, W.A., Gehre, M., Gröning, M., Meijer, H.A.J., Toman, B., Verkouteren, R.M., 2006. New Guidelines for $\delta^{13}C$ Measurements. Analytical Chemistry 78, 2439–2441.
Corso, J.D., Mietto, P., Newton, R.J., Pancost, R.D., Preto, N., Roghi, G., Wignall, P.B., 2012. Discovery of a major negative δ13C spike in the Carnian (Late Triassic) linked to the eruption of Wrangellia flood basalts. Geology 40, 79–82.
DeNiro, M.J., Epstein, S., 1978. Influence of diet on the distribution of carbon isotopes in animals. Geochimica et Cosmochimica Acta 42, 495–506.
Ershova, V.B., Ivleva, A.S., Podkovyrov, V.N., Khudoley, A.K., Fedorov, P.V., Stockli, D., Anfindon, O., Maslov, A.V., Khubanov, V., 2019. Detrital zircon record of the Mesoproterozoic to Lower Cambrian sequences of NW Russia: implications for the paleogeography of the Baltic interior. GFF 141, 1–10.
Fedorova, N.M., Levashova, N.M., Bazhenov, M.L., Meert, J.G., Sergeeva, N.D., Golovanova, I.V., Danukalov, K.N., Kuznetsov, N.B., Kadyrov, A.F., Khidiyatov, M. M., 2013. The East European Platform in the late Ediacaran: new paleomagnetic and geochronological data. Russian Geology & Geophysics 54, 1392–1401.
Fogel, M.L., Cifuentes, L.A., Velinsky, D.J., Sharp, J.H., 1992. Relationship of carbon availability in estuarine phytoplankton to isotopic composition. Marine Ecology Progress Series 82, 291–300.
Fox, C.P., Cui, X., Whiteside, J.H., Olsen, P.E., Summons, R.E., Grice, K., 2020. Molecular and isotopic evidence reveals the end-Triassic carbon isotope excursion is not from massive exogenous light carbon. Proceedings of the National Academy of Sciences 117, 30171–30178.
Freeman, K.H., 2001. Isotopic Biogeochemistry of Marine Organic Carbon. Reviews in Mineralogy and Geochemistry 43, 579–605.
Freeman, K.H., Hayes, J.M., Trendel, J.-M., Albrecht, P., 1990. Evidence from carbon isotope measurements for diverse origins of sedimentary hydrocarbons. Nature 343, 254–256.
Goryl, M., Marynowski, L., Brocks, J.J., Bobrovskiy, I., Derkowski, A., 2018. Exceptional preservation of hopanoid and steroid biomarkers in Ediacaran sedimentary rocks of the East European Craton. Precambrian Research 316, 38–47.
Grande, S.M.B.D., Neto, F.R.A., Mello, M.R., 1993. Extended tricyclic terpanes in sediments and petroleums. Organic Geochemistry 20, 1039–1047.
Grantham, P.J., Wakefield, L.L., 1988. Variations in the sterane carbon number distributions of marine source rock derived crude oils through geological time. Organic Geochemistry 12, 61–73.

Grazhdankin, D.V., Marusin, V.V., Meert, J., Krupenin, M.T., Maslov, A.V., 2011. Kotlin regional stage in the South Urals. Doklady Earth Sciences 440, 1222.
Grosjean, E., Love, G.D., Stalvies, C., Fike, D.A., Summons, R.E., 2009. Origin of petroleum in the Neoproterozoic-Cambrian South Oman Salt Basin. Organic Geochemistry 40, 87–110.
Hartnett, H.E., Keil, R.G., Hedges, J.I., Devol, A.H., 1998. Influence of oxygen exposure time on organic carbon preservation in continental margin sediments. Nature 391, 572–575.
Hayes, J.M., 1993. Factors controlling ^{13}C contents of sedimentary organic compounds: Principles and evidence. Marine Geology 113, 111–125.
Hayes, J.M., 2001. Fractionation of Carbon and Hydrogen Isotopes in Biosynthetic Processes. Reviews in Mineralogy and Geochemistry 43, 225–277.
Hayes, J.M., Freeman, K.H., Popp, B.N., Hoham, C.H., 1990. Compound-specific isotopic analyses: A novel tool for reconstruction of ancient biogeochemical processes. Organic Geochemistry 16, 1115–1128.
Holtvoeth, J., Whiteside, J.H., Engels, S., Freitas, F.S., Grice, K., Greenwood, P., Johnson, S., Kendall, I., Lengger, S.K., Lücke, A., Mayr, C., Naafs, B.D.A., Rohrssen, M., Sepúlveda, J., 2019. The paleolimnologist's guide to compound-specific stable isotope analysis – An introduction to principles and applications of CSIA for Quaternary lake sediments. Quaternary Science Reviews 207, 101–133.
Hoshino, Y., Poshibaeva, A., Meredith, W., Snape, C., Poshibaev, V., Versteegh, G.J.M., Kuznetsov, N., Leider, A., van Maldegem, L., Neumann, M., Naeher, S., Moczydłowska, M., Brocks, J.J., Jarrett, A.J.M., Tang, Q., Xiao, S., McKirdy, D., Das, S.K., Alvaro, J.J., Sansjofre, P., Hallmann, C., 2017. Cryogenian evolution of stigmasteroid biosynthesis. Science Advances 3, e1700887.
Hullar, M., Fry, B., Peterson, B.J., Wright, R.T., 1996. Microbial utilization of estuarine dissolved organic carbon: a stable isotope tracer approach tested by mass balance. Applied and Environmental Microbiology 62, 2489–2493.
Ivleva, A.S., Podkovyrov, V.N., Ershova, V.B., Anfinson, O.A., Khudoley, A.K., Fedorov, P.V., Maslov, A.V., Zdobin, D.Y., 2016. Results of U-Pb LA–ICP–MS dating of detrital zircons from Ediacaran-Early Cambrian deposits of the eastern part of the Baltic monoclise. Doklady Earth Sciences 468, 593–597.
Ivleva, A.S., Podkovyrov, V.N., Ershova, V.B., Khubanov, V.B., Khudoley, A.K., Sychev, S. N., Vdovina, N.I., Maslov, A.V., 2018. U-Pb LA–ICP–MS Age of Detrital Zircons from the Lower Riphean and Upper Vendian Deposits of the Luga-Ladoga Monocline. Doklady Earth Sciences 480, 695–699.
Jaraula, C.M.B., Grice, K., Twitchett, R.J., Böttcher, M.E., LeMetayer, P., Dastidar, A.G., Opazo, L.F., 2013. Elevated pCO2 leading to Late Triassic extinction, persistent photic zone euxinia, and rising sea levels. Geology 41, 955–958.
Kanzaki, Y., Murakami, T., 2018. Effects of atmospheric composition on apparent activation energy of silicate weathering: II. Implications for evolution of atmospheric CO_2 in the Precambrian. Geochimica et Cosmochimica Acta 240, 314–330.
Kelly, A.E., Love, G.D., Zumberge, J.E., Summons, R.E., 2011. Hydrocarbon biomarkers of Neoproterozoic to Lower Cambrian oils from eastern Siberia. Organic Geochemistry 42, 640–654.
Kodner, R.B., Pearson, A., Summons, R.E., Knoll, A.H., 2008. Sterols in red and green algae: quantification, phylogeny, and relevance for the interpretation of geologic steranes. Geobiology 6, 411–420.
Koga, Y., Nishihara, M., Morii, H., Akagawa-Matsushita, M., 1993. Ether polar lipids of methanogenic bacteria: structures, comparative aspects, and biosyntheses. Microbiological Reviews 57, 164–182.
Koga, Y., Morii, H., Akagawa-Matsushita, M., Ohga, M., 1998. Correlation of Polar Lipid Composition with 16S rRNA Phylogeny in Methanogens. Further Analysis of Lipid Component Parts. Bioscience, Biotechnology, and Biochemistry 62, 230–236.
Korkmaz, S., Kara-Gülbay, R., Khoitiyn, T., Erdoğan, M.S., 2022. Biomarkers geochemistry of the Alpagut oil shale sequence: an evaluation of dispositional environments and source rock potential from Dodurga-Çorum basin (N-Turkey). Journal of Petroleum Exploration and Production Technology 12, 2173–2189.
Krishna, M.S., Viswanadham, R., Prasad, M.H.K., Kumari, V.R., Sarma, V.V.S.S., 2018. Export fluxes of dissolved inorganic carbon to the northern Indian Ocean from the Indian monsoonal rivers. Biogeosciences 16, 505–519.
Kump, L.R., Arthur, M.A., 1999. Interpreting carbon-isotope excursions: carbonates and organic matter. Chemical Geology 161, 181–198.
Kump, L.R., Arthur, M.A., Patzkowsky, M.E., Gibbs, M.T., Pinkus, D.S., Sheehan, P.M., 1999. A weathering hypothesis for glaciation at high atmospheric pCO_2 during the Late Ordovician. Palaeogeography, Palaeoclimatology, Palaeoecology 152, 173–187.
Lan, C., Hong, Z., Ruizhong, H., Jiafei, X., Loung-Yie, T.L., Tien-Shun, L.A., Yanrong, Z., 2012. Paleoceanographic Indicators for Early Cambrian Black Shales from the Yangtze Platform, South China: Evidence from Biomarkers and Carbon Isotopes. Acta Geologica Sinica - English Edition 86, 1143–1153.
Lee, C., Fike, D.A., Love, G.D., Sessions, A.L., Grotzinger, J.P., Summons, R.E., Fischer, W.W., 2013. Carbon isotopes and lipid biomarkers from organic-rich facies of the Shuram Formation, Sultanate of Oman. Geobiology 11, 406–419.
Lee, C., Love, G.D., Fischer, W.W., Grotzinger, J.P., Halverson, G.P., 2015. Marine organic matter cycling during the Ediacaran Shuram excursion. Geology 43, 1103–1106.
Li, W.-P., Zhao, Y.-Y., Zhao, M.-Y., Zha, X.-P., Zheng, Y.-F., 2019. Enhanced weathering as a trigger for the rise of atmospheric O_2 level from the late Ediacaran to the early Cambrian. Scientific Reports 9, 10630.
Logan, G.A., Hayes, J.M., Hieshima, G.B., Summons, R.E., 1995. Terminal Proterozoic reorganization of biogeochemical cycles. Nature 376, 53–56.
Logan, G.A., Summons, R.E., Hayes, J.M., 1997. An isotopic biogeochemical study of Neoproterozoic and Early Cambrian sediments from the Centralian Superbasin, Australia. Geochimica et Cosmochimica Acta 61, 5391–5409.
Love, G.D., Grosjean, E., Stalvies, C., Fike, D.A., Grotzinger, J.P., Bradley, A.S., Kelly, A. E., Bhatia, M., Meredith, W., Snape, C.E., Bowring, S.A., Condon, D.J., Summons, R. E., 2009. Fossil steroids record the appearance of Demospongiae during the Cryogenian period. Nature 457, 718–721.
Martin, M.W., Grazhdankin, D.V., Bowring, S.A., Evans, D.A.D., Fedonkin, M.A., Kirschvink, J.L., 2000. Age of Neoproterozoic Bilatarian Body and Trace Fossils, White Sea, Russia: Implications for Metazoan Evolution. Science 288, 841–845.
Meidla, T., 2017. Ediacaran and Cambrian stratigraphy in Estonia: an updated review. Estonian Journal of Earth Sciences 66, 152.
Mens, K., Pirrus, E., 1997. Geology and Mineral Resources of Estonia: Vendian-Tremadocclastogenic sedimentation basins. Estonian Academy Pubishers 184–191.
Mills, B.J.W., Krause, A.J., Scotese, C.R., Hill, D.J., Shields, G.A., Lenton, T.M., 2019. Modelling the long-term carbon cycle, atmospheric CO_2, and Earth surface temperature from late Neoproterozoic to present day. Gondwana Research 67, 172–186.
Moldowan, J.M., Fago, F.J., Lee, C.Y., Jacobson, S.R., Watt, D.S., Slougui, N.-E., Jeganathan, A., Young, D.C., 1990. Sedimentary 12-n-Propylcholestanes, Molecular Fossils Diagnostic of Marine Algae. Science 247, 309–312.
Naafs, B.D.A., Bianchini, G., Monteiro, F.M., Sánchez-Baracaldo, P., 2022. The occurrence of 2-methylhopanoids in modern bacteria and the geological record. Geobiology 20, 41–59.
Pagani, M., Arthur, M.A., Freeman, K.H., 1999. Miocene evolution of atmospheric carbon dioxide. Paleoceanography 14, 273–292.
Pagani, M., Zachos, J.C., Freeman, K.H., Tipple, B., Bohaty, S., 2005. Marked Decline in Atmospheric Carbon Dioxide Concentrations During the Paleogene. Science 309, 600–603.
Pagès, A., Schmid, S., Edwards, D., Barnes, S., He, N., Grice, K., 2016. A molecular and isotopic study of palaeoenvironmental conditions through the middle Cambrian in the Georgina Basin, central Australia. Earth and Planetary Science Letters 447, 21–32.
Pancost, R.D., Damsté, J.S.S., 2003. Carbon isotopic compositions of prokaryotic lipids as tracers of carbon cycling in diverse settings. Chemical Geology 195, 29–58.
Pancost, R.D., Freeman, K.H., Herrmann, A.D., Patzkowsky, M.E., Ainsaar, L., Martma, T., 2013. Reconstructing Late Ordovician carbon cycle variations. Geochimica et Cosmochimica Acta 105, 433–454.
Paszkowski, M., Budzyń, B., Mazur, S., Sláma, J., Środoń, J., Millar, I.L., Shumlyanskyy, L., Kędzior, A., Liivamägi, S., 2021. Detrital zircon U-Pb and Hf constraints on provenance and timing of deposition of the Mesoproterozoic to Cambrian sedimentary cover of the East European Craton, part II: Ukraine. Precambrian Research 362, 106282.
Pearson, A., Page, S.R.F., Jorgenson, T.L., Fischer, W.W., Higgins, M.B., 2007. Novel hopanoid cyclases from the environment. Environmental Microbiology 9, 2175–2188.
Pearson, A., 2010. Handbook of Hydrocarbon and Lipid Microbiology. Springer, pp. 143–156.
Pehr, K., Love, G.D., Kuznetsov, A., Podkovyrov, V., Junium, C.K., Shumlyanskyy, L., Sokur, T., Bekker, A., 2018. Ediacara biota flourished in oligotrophic and bacterially dominated marine environments across Baltica. Nature Communications 9, 1807.
Pirrus, E., 1992. Freshening of the Late Vendian Basin on the East European Craton. Proceedings of the Estonian Academy of Sciences Geology 41, 115–123.
Popp, B.N., Laws, E.A., Bidigare, R.R., Dore, J.E., Hanson, K.L., Wakeham, S.G., 1998. Effect of Phytoplankton Cell Geometry on Carbon Isotopic Fractionation. Geochimica et Cosmochimica Acta 62, 69–77.
Poulton, S., 2021. Elements in Geochemical Tracers in Earth System Science: The Iron Speciation Paleoredox Proxy. Cambridge University Press, Cambridge.
Poulton, S.W., Canfield, D.E., 2005. Development of a sequential extraction procedure for iron: implications for iron partitioning in continentally derived particulates. Chemical Geology 214, 209–221.
Poulton, S.W., Canfield, D.E., 2011. Ferruginous Conditions: A Dominant Feature of the Ocean through Earth's History. Elements 7, 107–112.
Poulton, S.W., Fralick, P.W., Canfield, D.E., 2004. The transition to a sulphidic ocean ~ 1.84 billion years ago. Nature 431, 173–177.
Raiswell, R., Canfield, D.E., 1998. Sources of iron for pyrite formation in marine sediments. American Journal of Science 298, 219–245.
Raiswell, R., Newton, R., Wignall, P.B., 2001. An Indicator of Water-Column Anoxia: Resolution of Biofacies Variations in the Kimmeridge Clay (Upper Jurassic, U.K.). Journal of Sedimentary Research 71, 286–294.
Reinfelder, J.R., 2011. Carbon Concentrating Mechanisms in Eukaryotic Marine Phytoplankton. Annual Review of Marine Science 3, 291–315.
Roeske, C.A., O'Leary, M.H., 1984. Carbon isotope effects on enzyme-catalyzed carboxylation of ribulose bisphosphate. Biochemistry 23, 6275–6284.
Rohmer, M., Bouvier-Nave, P., Ourisson, G., 1984. Distribution of Hopanoid Triterpenes in Prokaryotes. Microbiology 130, 1137–1150.
Rohrssen, M., Love, G.D., Fischer, W., Finnegan, S., Fike, D.A., 2013. Lipid biomarkers record fundamental changes in the microbial community structure of tropical seas during the Late Ordovician Hirnantian glaciation. Geology 41, 127–130.
Rontani, J.-F., Volkman, J.K., 2005. Lipid characterization of coastal hypersaline cyanobacterial mats from the Camargue (France). Organic Geochemistry 36, 251–272.
Roussel, A., Cui, X., Summons, R.E., 2020. Biomarker stratigraphy in the Athel Trough of the South Oman Salt Basin at the Ediacaran-Cambrian Boundary. Geobiology 18, 663–681.
Schwark, L., Empt, P., 2006. Sterane biomarkers as indicators of palaeozoic algal evolution and extinction events. Palaeogeography, Palaeoclimatology, Palaeoecology 240, 225–236.
Scott, K.M., Schwedock, J., Schrag, D.P., Cavanaugh, C.M., 2004. Influence of form IA RubisCO and environmental dissolved inorganic carbon on the $\delta^{13}C$ of the clam-

chemoautotroph symbiosis Solemya velum. Environmental Microbiology 6, 1210–1219.
Sliaupa, S., Fokin, P., Lazauskiene, J., Stephenson, R.A., 2006. The Vendian-Early Palaeozoic sedimentary basins of the East European Craton 32, 449–462.
Smith, K.S., Jakubzick, C., Whittam, T.S., Ferry, J.G., 1999. Carbonic anhydrase is an ancient enzyme widespread in prokaryotes. Proceedings of the National Academy of Sciences 96, 15184–15189.
Soldatenko, Y., Albani, A.E., Ruzina, M., Fontaine, C., Nesterovsky, V., Paquette, J.L., Meunier, A., Ovtcharova, M., 2019. Precise U-Pb age constrains on the Ediacaran biota in Podolia, East European Platform. Ukraine. Scientific Reports 9, 1675.
Stolper, D.A., Bucholz, C.E., 2019. Neoproterozoic to early Phanerozoic rise in island arc redox state due to deep ocean oxygenation and increased marine sulfate levels. Proceedings of the National Academy of Sciences 116, 8746–8755.
Wakeham, S.G., Lewis, C.M., Hopmans, E.C., Schouten, S., Damsté, J.S.S., 2003. Archaea mediate anaerobic oxidation of methane in deep euxinic waters of the Black Sea. Geochimica et Cosmochimica Acta 67, 1359–1374.
Wang, N., Li, M., Hong, H., Song, D., Tian, X., Liu, P., Fang, R., Chen, G., Wang, M., 2019. Biological sources of sedimentary organic matter in Neoproterozoic-Lower Cambrian shales in the Sichuan Basin (SW China): Evidence from biomarkers and microfossils. Palaeogeography, Palaeoclimatology, Palaeoecology 516, 342–353.
Wood, R.A., Poulton, S.W., Prave, A.R., Hoffmann, K.-H., Clarkson, M.O., Guilbaud, R., Lyne, J.W., Tostevin, R., Bowyer, F., Penny, A.M., Curtis, A., Kasemann, S.A., 2015. Dynamic redox conditions control late Ediacaran metazoan ecosystems in the Nama Group, Namibia. Precambrian Research 261, 252–271.
Zhang, J., Quay, P.D., Wilbur, D.O., 1995. Carbon isotope fractionation during gas-water exchange and dissolution of CO_2. Geochimica et Cosmochimica Acta 59, 107–114.
Zumberge, J.E., 1987. Prediction of source rock characteristics based on terpane biomarkers in crude oils: A multivariate statistical approach. Geochimica et Cosmochimica Acta 51, 1625–1637.
Zumberge, J.A., Rocher, D., Love, G.D., 2020. Free and kerogen-bound biomarkers from late Tonian sedimentary rocks record abundant eukaryotes in mid-Neoproterozoic marine communities. Geobiology 115, 246.